4.1 Introduction

Semisolid processing of aluminum alloys has attracted significant interest because it combines the advantages of both conventional forming techniques such as casting and forging. Also, the results in superior microstructural characteristics with commensurate physical and mechanical properties. The process offers several potential advantages such as lower operating temperatures, laminar flow during mould filling and low shrinkage porosity. It ensures longer die life, reduced gas entrapment, good surface finish and low energy consumption.[Flemings, 1991]

This process produces globular morphology of the primary phase due to which improve mechanical properties of the alloys. Although semisolid processing is relatively expensive as compared to the conventional casting method. The conventional casting usually ends up with defects like shrinkage and porosity which are absent in semisolid processing routes. Owing to the advantages offered by the semisolid processing route, several such techniques have been developed so far, such as Rheocasting, Thixocasting, Magneto hydrodynamic method, each with their own advantages and limitations. Rheocasting was originally developed by Spencer [Spencer et al. 1972] in 1970 at MIT. It involves the conversion of liquid into a semisolid slurry of 30 to 65 % solid which is injected into the die. In addition, Fan[Fan, 2002] reported that Rheocasting produce near-net shape castings with improved mechanical properties and better service life due to lower processing temperatures.

However, electrical stirring is not suitable for large ingots (>80 mm) due to the limitation of depth of the magnetic field produced.[Rishu et al. 2014]. On the other hand, Magneto hydrodynamic (MHD) route involves stirring the metal electromagnetically in semi-solid state to break up the dendrites and is a much better process for producing critical components with good mechanical properties.

Although, semi-solid Rheocasting (SSR) route involves relatively lower processing cost as compared to the MHD process. Further, SSR process produces relatively inferior mechanical properties than that of MHD manufactured components. Mohammed et al.[Mohammed et al. 2013] reported that the cooling slope method is simple than that of other Rheocasting techniqes, but not suitable for critical applications. However, Rheocasting has some limitations like high production costs, low productivity and suitable for limited alloy systems.[Guo and yang, 2007]. In contrast, Thixocasting involves deforming the semi-solid slurry directly into a near-net shape product. Thus, Thixocasting process is a complex process and requires a feed stock of well-controlled properties rendering it expensive.[Das Gupta et al. 2004 and Jorstad et al. 2004]. The strain induced melt activation(SIMA) process has been developed by Young[Young et al. 1982 and Xia et al. 2005] in the 1980's which produces globular primary α-phase in the semi-solid microstructure.

The SIMA process involves the following steps: (a) casting of alloy in convenient sizes to get a dendritic structure (b) strain energy is induced by forging or a similar high-deformation process like extrusion, rolling etc. (c) the deformed billet is heated to semi-solid state where recrystallisation occurs and liquid metal penetrates in the recrystallized grain boundaries thus resulting solid globular particles surrounded by liquid. [Alipour et al. 2013]. The cast alloy is subjected to cold working to generate defects structures and their beneficial effects are utilised in recrystallization of solid fraction during inter critical annealing. A cast product cannot sustain high deformation without cracking, hence warm working is necessary to achieve better plastic flow of the material. However in this process defect structures are partially annihilated and only remaining defects facilitate recrystallisation of solid fraction during intercritical annealing. SIMA process is mostly considered as an ideal method for semi-solid process and frequently researched in fabricating semi-solid aluminium and zinc alloys. [Wang et al. 2008]. Sahoo et al. [Sahoo et al. 2009] reported that A 356 aluminum alloy cannot be cold rolled due to low ductility at room temperature. Hence, warm rolling(temperature 300 °C) was carried out. In contrast, Choi et al. [Choi et al. 1998] globularization of aluminium 2024 alloy merely by cold working in the SIMA process. In recent years, SIMA process has been used to improve the mechanical and tribological properties. The advantages of SIMA compared to mechanical stirring as well as magneto hydro dynamic stirring are (a) it is applicable to both low and high melting point alloys[Czerwinski et al. 2003] (b) this process reduced the oxidation and combustion problems of magnesium alloy to attain the pure alloy and helps to make the semisolid thixocasting/rheocasting easily. One can get the desired mechanical properties by achieving the globular morphology of the primary α-phase of the alloy. The factors affecting the size and shape of the globular morphology are degree of deformation, the semi-solid annealing temperature and the soaking time. [Flemings et al. 1991, Kirkwood et al. 1994 and Sang-Yong et al. 2001]. The stirring the semi-solid slurry is necessary to decrease the apparent viscosity as compared to undisturbed slurries [Spencer et al. 1972]. The final microstructure consists of dendrite-free equiaxed grains with globular morphology, which result in good mechanical properties [Flemings et al. 1991]. However, Al 2024 alloy was also produced by semi-solid process., But, it has a very narrow semisolid region-so that it is difficult to work in such a region. Therefore, It is important to design the new alloys whose semi-solid temperature range is wide so that full advantage of semi-solid processing can be taken. To solve this problem, the Al -10Cu-Fe alloy was designed as it has a higher semisolid temperature range and making it more suitable for semisolid forming. Aluminium-copper alloy containing 9 to 11% Cu possesses offer limited use in aircraft cylinder heads and in automotive pistons and cylinder blocks. [Kearney et al. 1990]. This alloy is difficult to work material and spheroidization of the primary phase is highly desirable in its fabrication and which has not been studied systematically so far for this material during semi-solid processing, particularly the influence of resulting microstructure on the tribological properties. This forms the central aim of this study to produce a fine globular microstructure of the Al-10Cu alloy feedstock suitable for semisolid forming and study the microstructure, mechanical and tribological properties of the SIMA processed alloy casts and compared with those of conventional metal mould casting.

4.2 Experimental details

4.2.1 Preparation of Metal Mould Casting

The Al-10Cu alloy was prepared by melting the commercial purity Al and Cu in a graphite crucible using an electric resistance heating furnace. The melt was then poured into a preheated (300 ºC) rectangular cast iron mould at a pouring temperature 700 ºC for producing an as-cast dendritic structure. The final chemical composition of the resulting alloy (Si:0.686, Fe:0.615, Cu:10, Mn:0.082, Zn:0.655, Pb:0.0190 and balance Al, all in wt%).

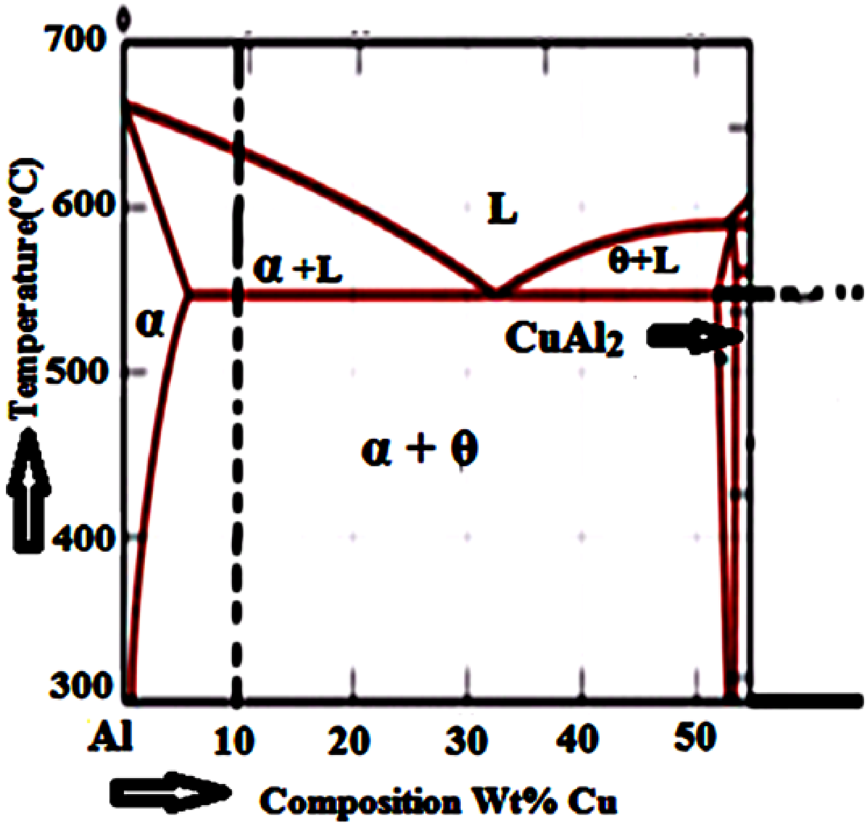

Figure 4.1: Al-Cu phase diagram

4.2.2. Solidification temperature range

Al-Cu phase diagram has shown in the figure 4.1. A differential scanning calorimeter (DSC) was used to determine the melting point and the solidification temperature range of the Al-10Cu alloy. DSC results showed the liquidus and the solidification temperature range of the alloy were 636 and 546 °C respectively (Figure 4.2).

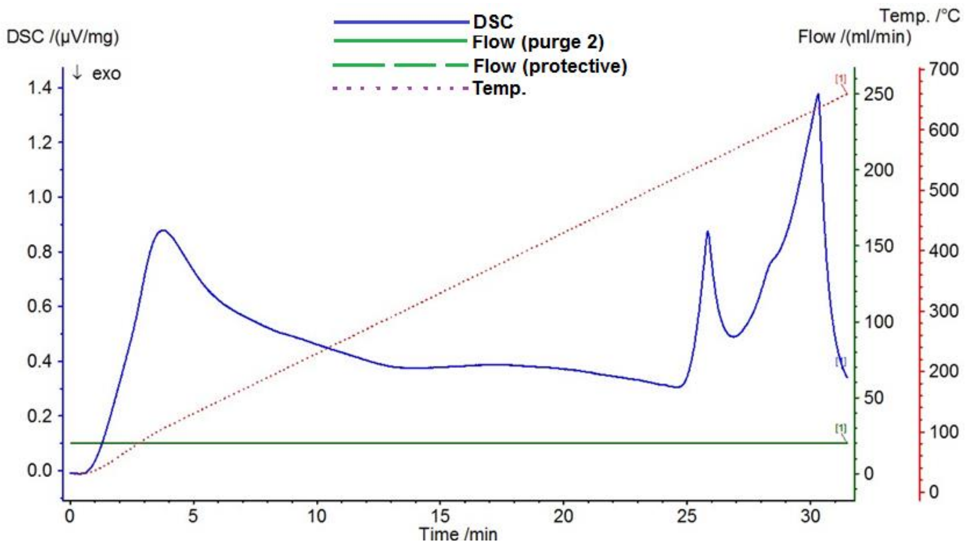

Figure 4.2: DSC measurement of Al-10Cu Alloy.

4.2.3. Preparation of Stirred Metal Mould Casting (SC)

A vertical muffle furnace with programmable temperature and stirring controls and bottom pouring arrangements has been used. To achieve chemical and thermal homogeneity, the alloy melt was stirred for about 20 minutes using a graphite stirrer to avoid melt the contamination, which is a very common problem with metallic stirrers. Argon gas was supplied to avoid the formation of an oxide layer on the surface of the metal. The alloy was poured at 700 °C into the cast iron metal mold which was preheated at 300 °C shown in the figure 4.3.

4.2.4. SIMA processing technique

The samples were cut into 60 mm x 55 mm x 20 mm rectangular blocks from the ingot and subjected to warm forging after annealing at 300 °C for 45 minutes in a electric resistance furnace. The Al-10Cu alloy was plastically deformed to a thickness reduction of 50% obtained by warm forging to induce sufficient energy stored in the alloy. It acts as a driving force for recovery and recrystallization process. The amount of strain induced during this process was significant and provided driving force to form the globular grains of the primary phase when the strained alloy was subjected to the semi solid region heat treatment followed by water quenching. This deformed piece was again cut into convenient sizes, and the samples were placed in the electric muffle furnace to held at a semisolid temperature, followed by water quenching. The holding time has been varied for the samples ranging from 10 to 55 minutes at the temperature 580 °C. The cylindrical specimens of 8 mm in diameter and 30 mm in length were prepared by machining the alloy cast.

4.2.5. Metallography procedures

MMC and SC subjected to SIMA process samples were prepared using standard metallographic procedure of grinding and polishing. Samples were polished first on emery papers (1/0, 2/0, 3/0, and 4/0) followed by disc cloth polishing using brasso and kerosene and lastly with diamond paste to get the mirror scratch free finish. These samples were etched with Keller's reagent (1% Vol.. HF, 1.5%Vol. HCl, 2.5% Vol..HNO_3 and balance water) and examined under a Leitz Metallux-3 optical microscope.

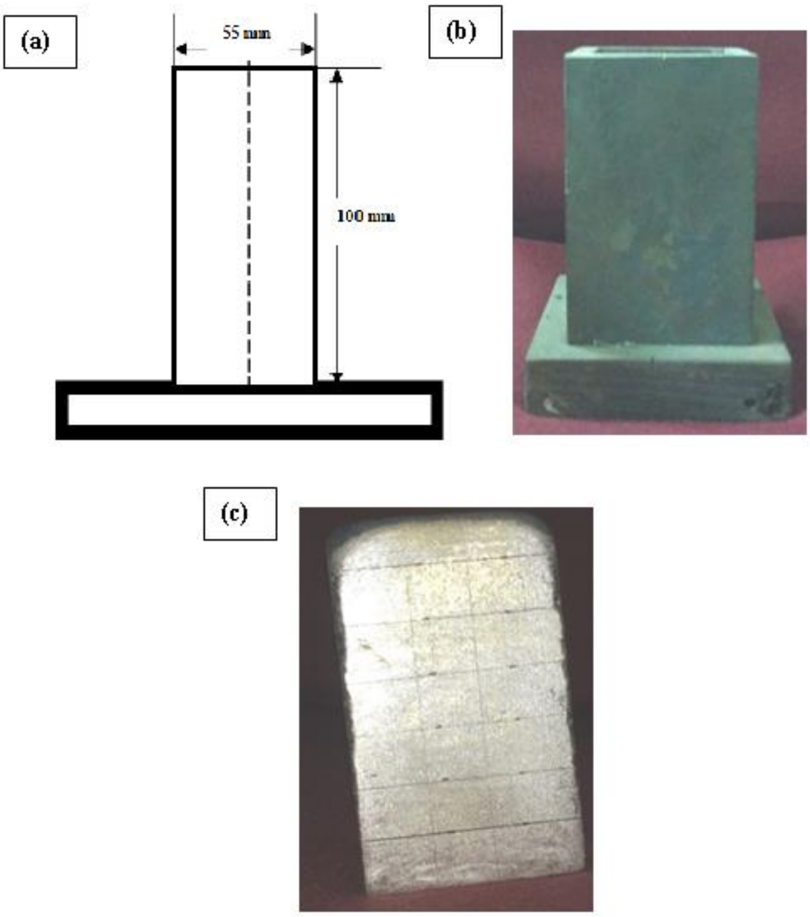

Figure 4.3: Metal Mould (a) schematic diagram, (b) picture, (c) casting sample

4.2.6. Mechanical Testing

Tensile and hardness tests were carried out at room temperature. Instron Machine with a crosshead speed of 1mm/minute was used for finding the ultimate tensile strength of the samples according to BS12-1950 standard. The schematic diagram and picture of the tensile sample is shown in the Figure 4.4. Scanning electron microscopy Jeol 840A operated at 15 kV was used to examine the fracture surface of the tensile samples.

Alloy cast samples were polished and cleaned with acetone for conducting the hardness testing using LECOLV700AT Vickers hardness tester at a load of 5 kg. The average Vickers hardness value is obtained from the five measurements for each sample.

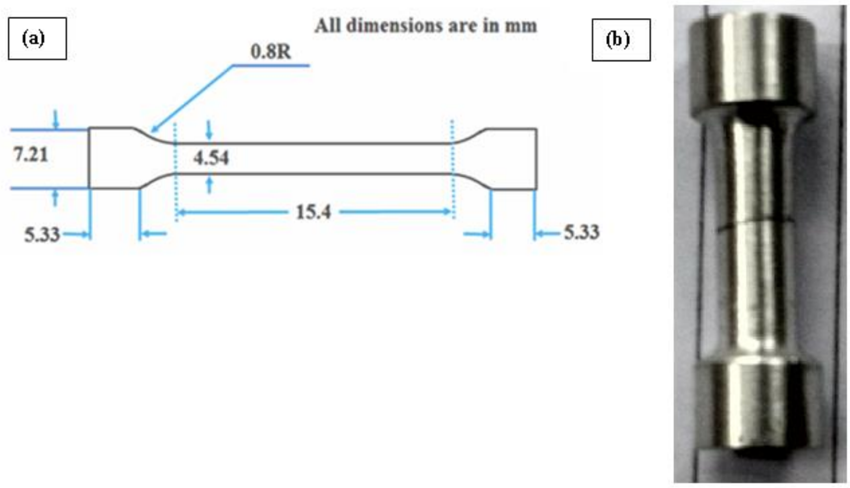

Figure 4.4: Tensile testing sample (a) schematic diagram, (b) picture.

4.2.7. Wear Testing procedures

Wear testing of the alloy casts, subjected to different processing methods, was carried out by DUCOM pin-on-disc-type wear-test-machine at 10 to 40 N applied load, 1 m/s sliding speed to a sliding distance of 3600 m. Wear pin specimens of 8 mm in diameter and 30 mm length were prepared from the central portion of the castings were held against EN 31 steel disc 60 HRC shown in the figure 4.5. The surfaces of the pin and disc were ground to a constant surface finish of about 0.4 µm. The sample was cleaned with acetone by using ultrasonic cleaner and weighed to an accuracy of ± 0. 1 mg before testing and at every 10 min intervals.

Standard procedure was followed in conducting the wear test to get accurate results. The average volume of wear from a sliding distance of 3600 m was calculated from the average weight loss of three test pins before and after the experiment. Volume loss was calculated by the weight loss and density measurement of the samples using Archimedes' principle. Friction force was monitored using load cell attached to the wear testing machine. The worn surfaces were investigated under SEM (ZEISS Model-EVO 18) and 3D-profilometer from Rtec Instruments.

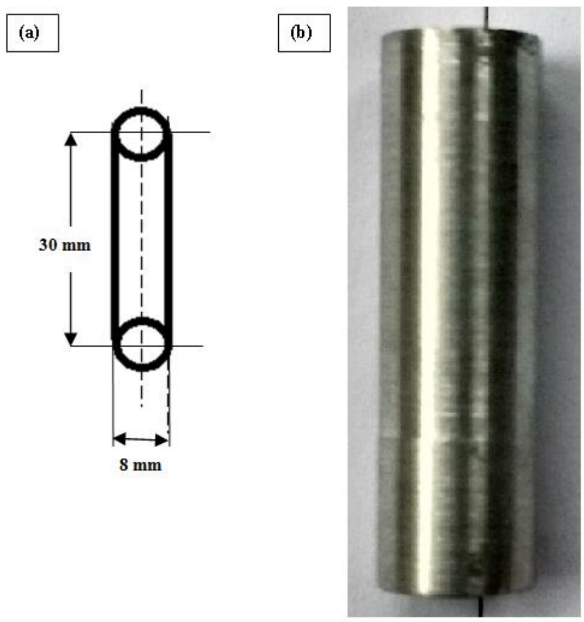

Figure 4.5: Wear testing sample (a) schematic diagram, (b) picture.

4.3 Results and Discussion

4.3.1 Microstructral Features

The microstrctural changes occurred in two successive steps of pre-deformation (50%) and partial melting of alloy at 580 °C with varying holding time from 10 to 55 minutes followed by water quenching. Figure 4.6a shows the optical microstructure of the metal mould casting of the Al-10Cu alloy, which exhibits the fully dendritic structure of α-Al. As expected, the microstructure of the SIMA processed samples are different from that of the metal mould cast alloy. The dendritic morphology of the primary phase of the alloy which produced by MMC was changed to largely globular with small differences in grain size. Hassas-Irani et al. [Hassas-Irani et al. 2013] reported that the semisolid deformation behavior of the thixoformed material depends on their initial microstructures. . The primary α-phase at 580 ºC for 10 minutes holding time was neither completely isolated by a continuous liquid nor spheroized which is shown in the figure 4.6b. However, with increase in holding time from 10 to 30 minutes, the primary α - phase was isolated from the liquid shown in Figure 4.6c. On further increasing the holding time to 40 minutes, the primary phase started coarsening which was shown in the Figure 4.6d.

The coarsening of globular primary α - phase is continued further with increasing the holding time to 45 and also for 55 minutes whose resultant microstructures were shown in the Figure 4.6e and 4.6f. Figure 4.7a – 4.7e show the grain distribution of the SIMA processed alloy with varying holding times from 10 to 55 minutes. Figure 4.8 shows the globular primary α - phase with some liquid droplets can be seen which were entrained in the primary grains. The distribution of the globular primary α - phase is shown below the micrograph. As can be seen from the figure, while the stirred MMC cast subjected to the SIMA process have shown fine average size of the primary α - phase (45 µm), the ones subjected to MMC to SIMA had shown large average size of primary α - phase (65 µm). Freitas et al.[Freitas et al. 2004] reported that the primary α - phase with sizes smaller than 100 µm were leaded the favorable microstructure for thixoforming and SIMA process. The SIMA process is popular as compared to other stirring methods of semisolid processing because the process does not require complicated equipment. The uniform fine globular microstructure could obtained by this process. SIMA process involves four stages: (a) Initially, the alloy is cast into convenient size to get the dendritic microstructure (b) then the cast alloy subjected to hot working to get the directional properties and to reduce the thickness of the casting (c), further, the alloy is subjected to cold working to induce the strain which is primary requirement of the SIMA process (d) finally, the alloy is partially remelted in the range 15 - 50 vol. % liquid and held isothermally for a short time to get equiaxed microstructure. The process involved deformation of a cast alloy at low temperature. This effects result in high density of crystal defects which provide driving force for recrystallization of the primary solid phase during their inter-critical annealing in two phase semi-solid regions. The eutectic at this stage melts and liquid enter into a grain boundary region of the recrystallized grains with a time of annealing, the grains are isolated and spherodize giving rise to spherical morphologies of the forming phase. Nevertheless, coarsening of the primary phase in subject to the prolonged time of annealing.[Doherty et al.1984] This is evident from the micrographs shown in Figure 4.6.

The microstructure of stirred MMC subjected to SIMA process has shown many interesting points like the dendritic structure of the MMC converted to globular primary phase of α, eutectic phase is distributed uniformly in the matrix and some droplets of eutectic phase are entrained into the primary phase. The improved wear properties of Al-10Cu alloy have been observed due to their uniform distribution of eutectic phase liquid droplets in the solid matrix.[Rao et al. 2016] In addition, the droplets entrained in the primary phase due to repeated thermal cycling of the alloy. However, the number of droplets entrained in the primary phase during the SIMA process of stirred metal mould casting is less compared to previous studies. .[Rao et al. 2016] This may be due to single thermal cycling of the SIMA process. MMC subjected to SIMA process has not shown the significant quantity of droplets as compared to stirred MMC subjected to SIMA process and the clustering of the eutectic (or) intermetallic phase can be seen in the microstructure. This may be due to non stirring of the metal before pouring into the die. The mechanism of microstructural evolution is considered to give rise to various size and size distribution of the primary phase. The clustering of the eutectic or intermetallic phase can be seen in the microstructure, this could be due to lacking of stirring the liquid metal before pouring into the metal die. Thus, the stirring of the melt is an important process parameter for the distribution of the intermetallics in the in-situ composites.

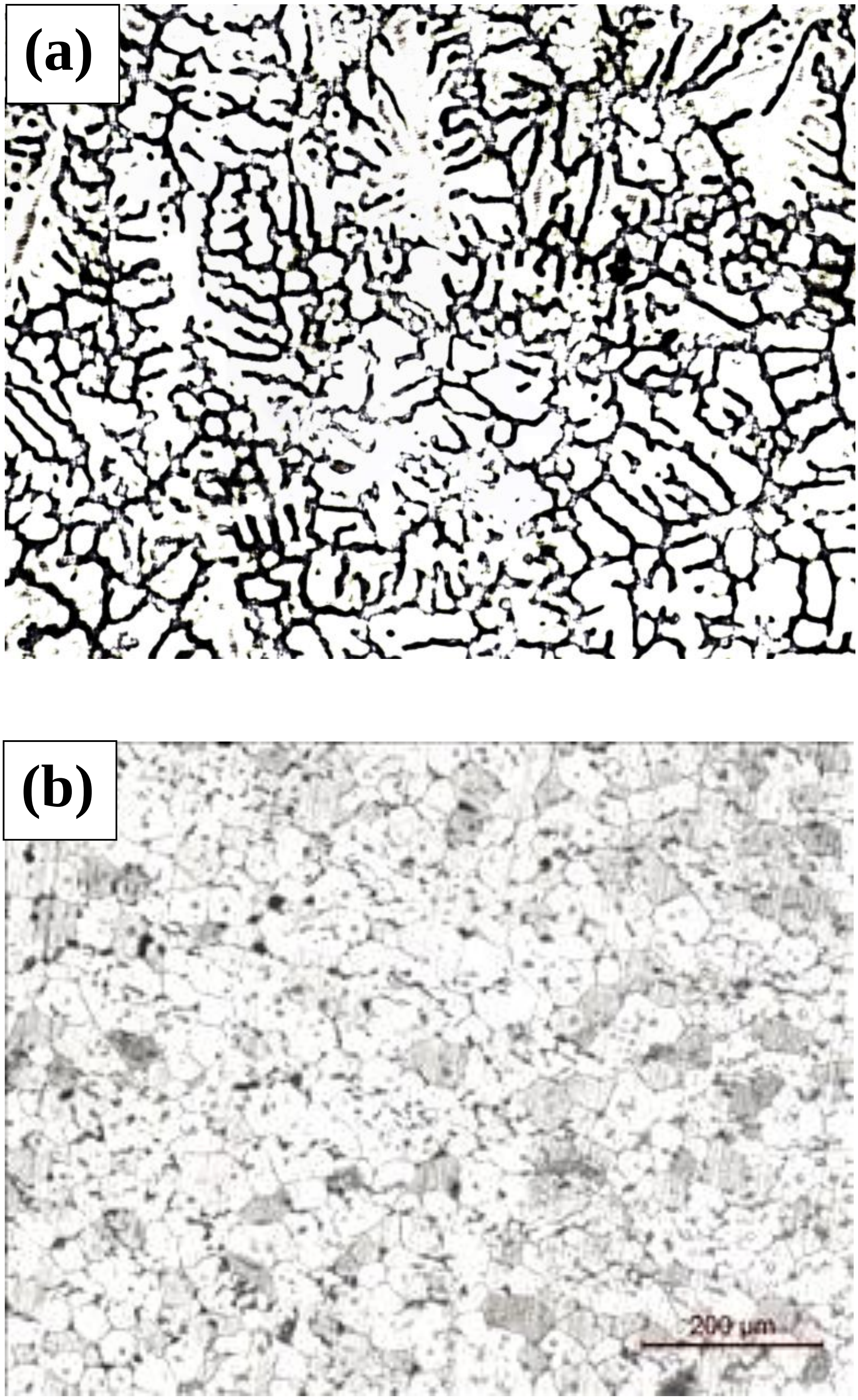
(a)
(b)
200 µm

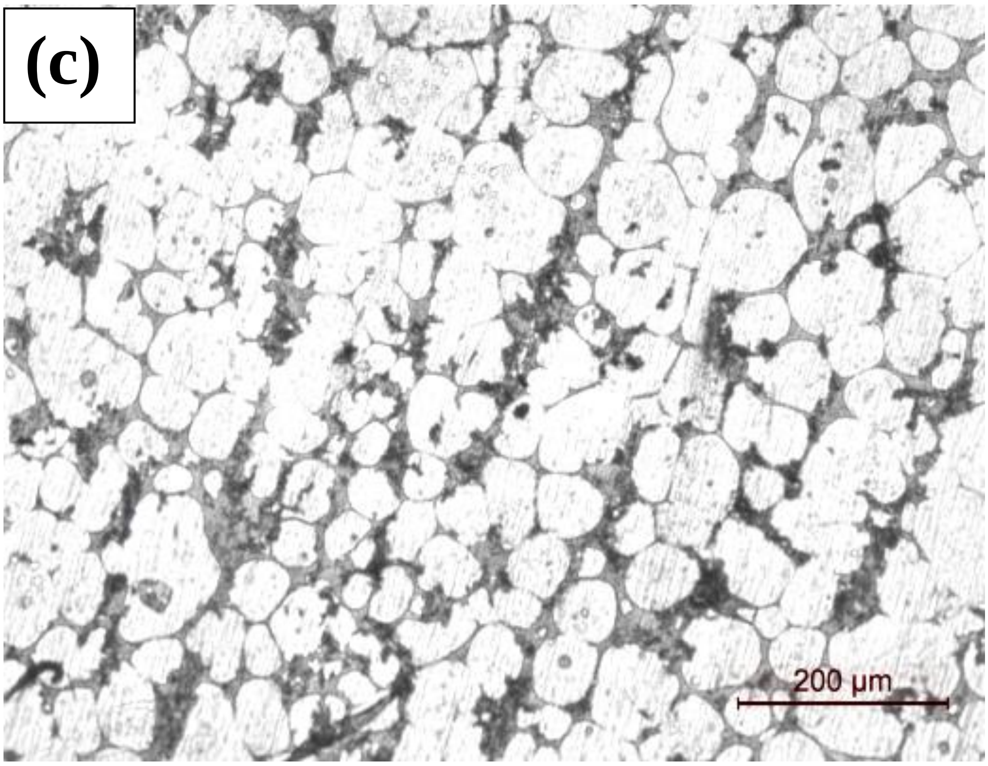
(c)
200 µm

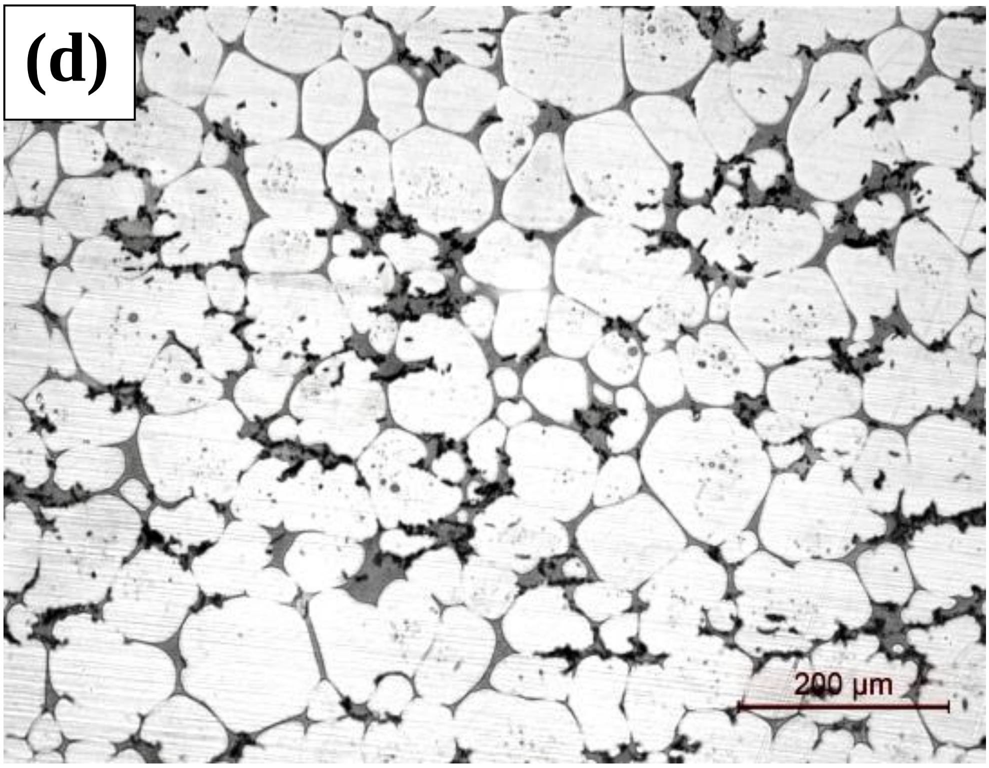
(d)
200 µm

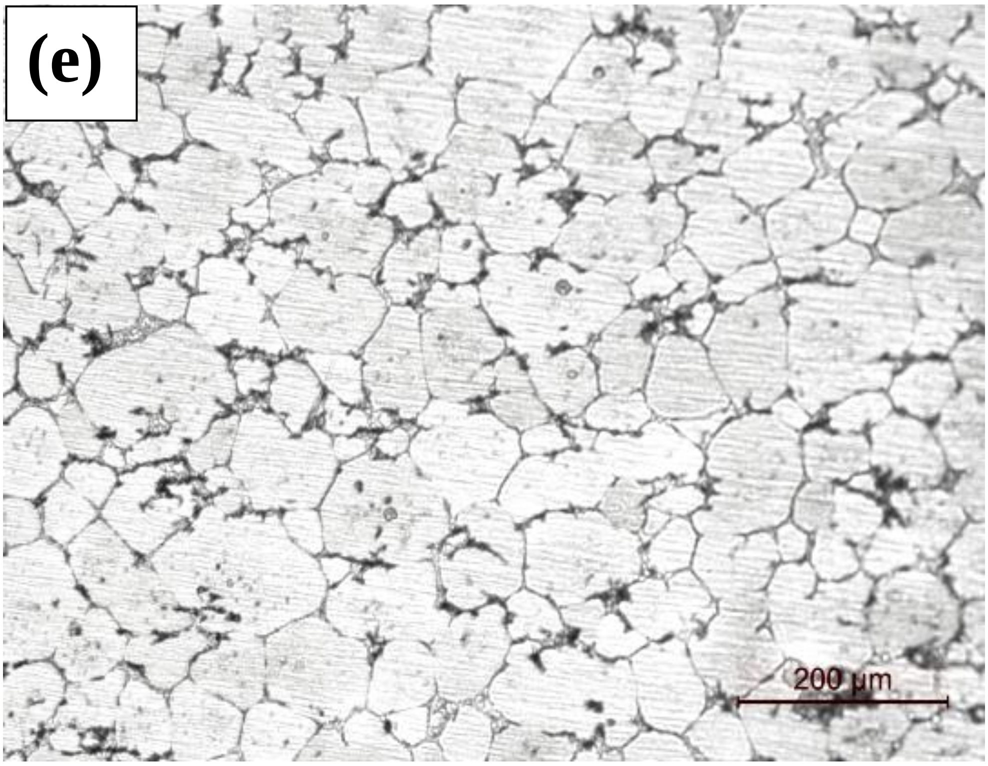

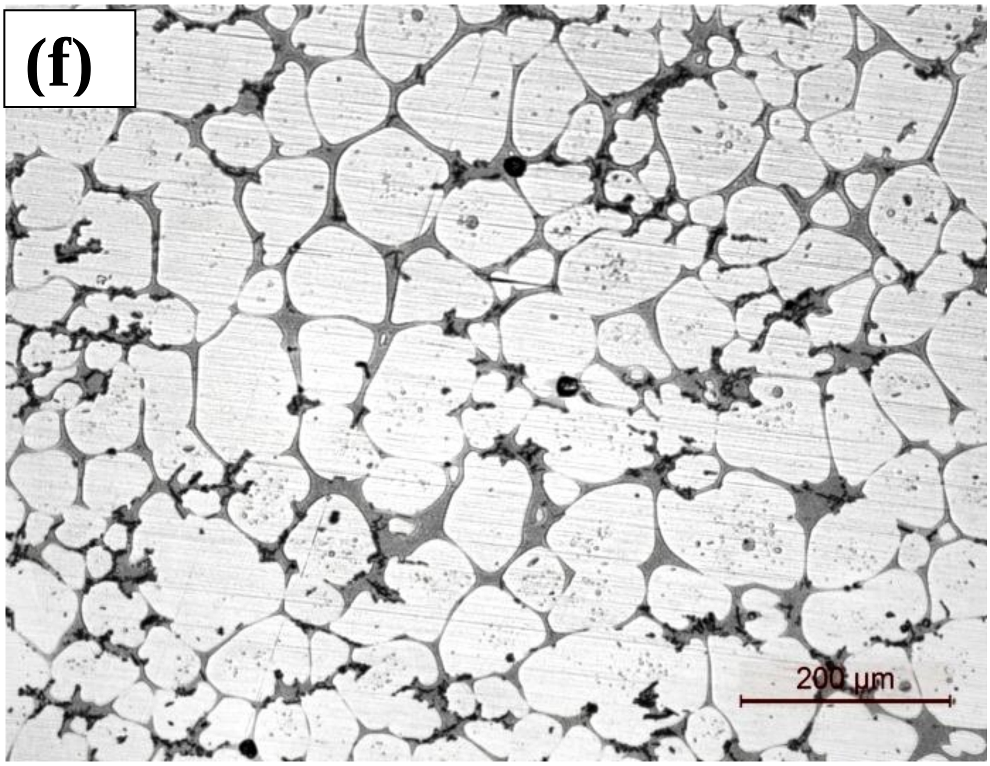

Figure 4.6: Optical Micrographs of Al-10Cu alloy (a) Metal Mould Casting, (b)-(f) SIMA processed sample at 580 °C. The holding times for (b) to (f) are 10, 30, 40, 45, and 55 minutes respectively.

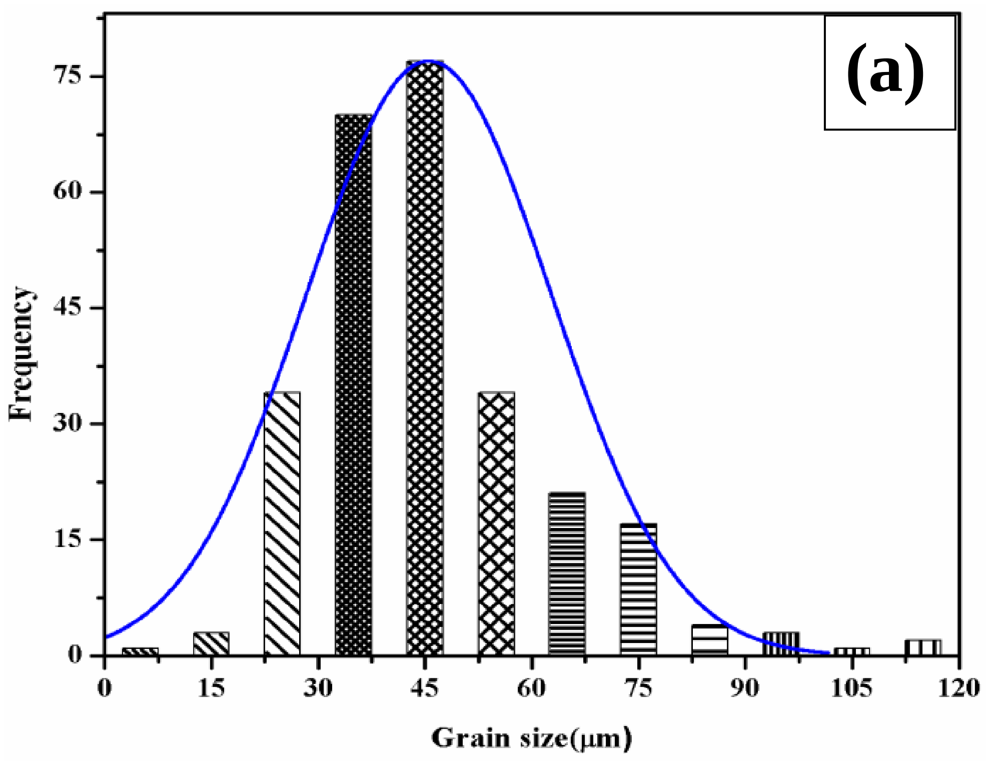
(a)
Frequency
0
15
30
45
60
75
0 15 30 45 60 75 90 105 120
Grain size(μm)

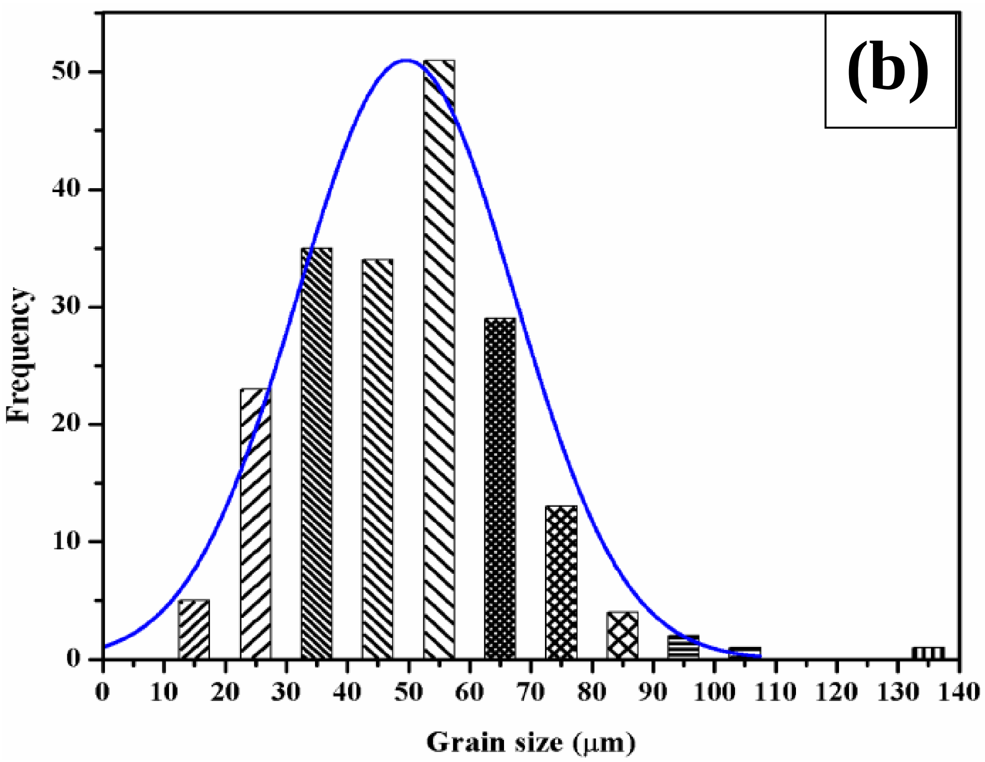
(b)
Frequency
0
10
20
30
40
50
0 10 20 30 40 50 60 70 80 90 100 110 120 130 140
Grain size (μm)

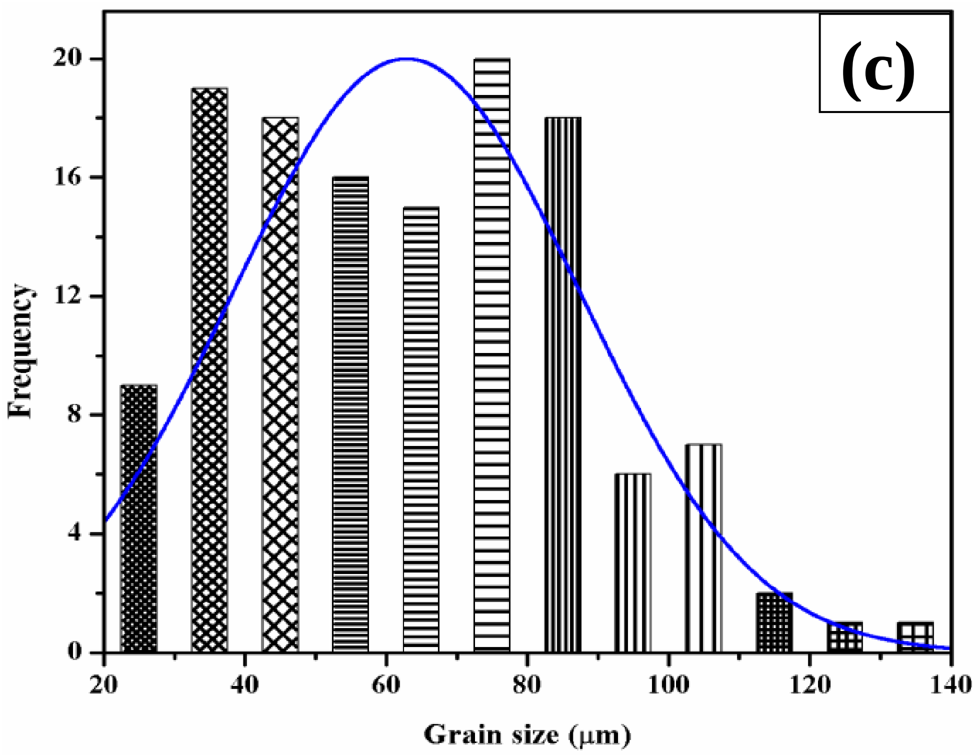
(c)
Frequency
0
4
8
12
16
20
20
40
60
80
100
120
140
Grain size (μm)

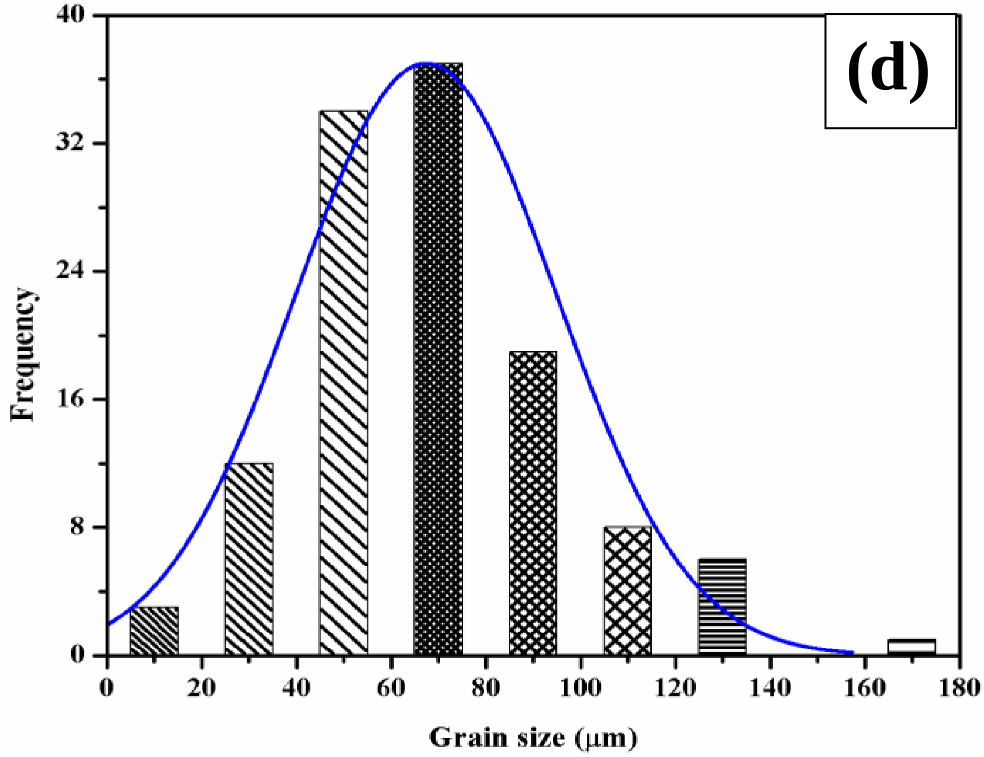
(d)
Frequency
0
8
16
24
32
40
0
20
40
60
80
100
120
140
160
180
Grain size (μm)

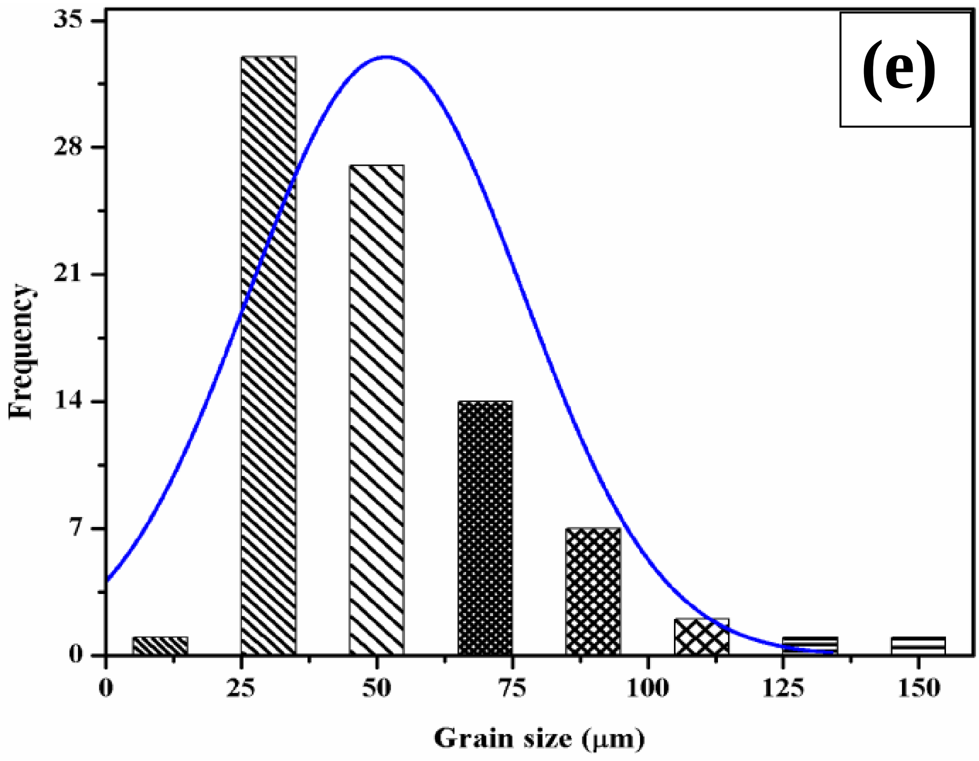

Figure 4.7: Grain size distribution of SIMA processed samples of Al-10Cu alloy at 580 °C with holding times (a) 10 minutes, (b) 30 minutes, (c) 40 minutes, (d) 45 minutes and (e) 55 minutes. These correspond to the microstructures in Fig. 2(b)-(f).

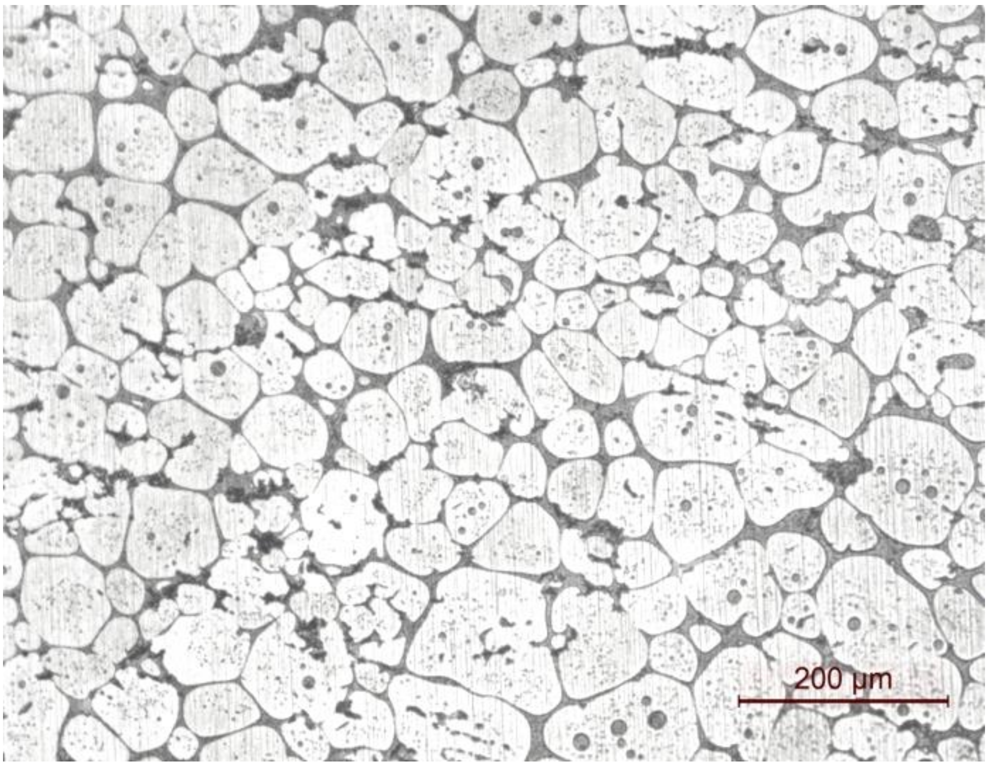

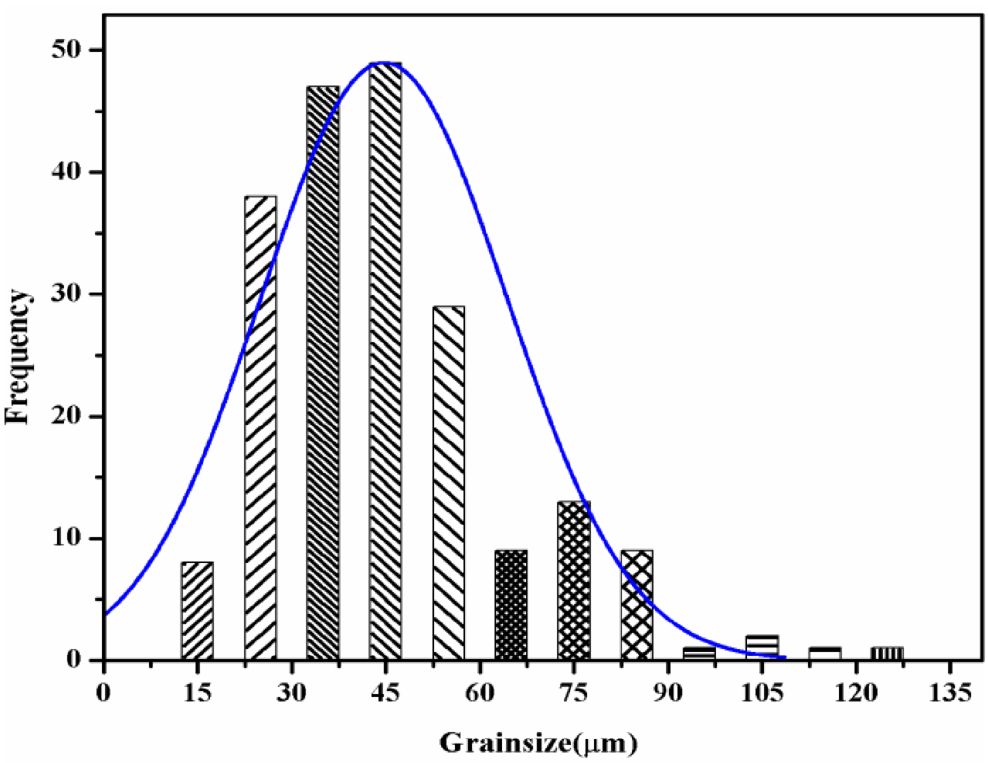

Figure 4.8: Optical microscopy and grain distribution of SIMA processed Al-10Cu alloy sample at 580 °C with holding time 30 minutes of stirred MMC.

The grain boundaries were enriched with alloying elements during the its partial melting and it was confirmed by the EDS analysis (Fig. 4.9). The EDS-line analysis of stirred MMC subjected to the SIMA process at grain boundary and in the grain are shown in Figure 4.10 and 4.11 respectively. It is clear from these figures that the segregation of solute occurred at high concentration of Cu and Fe in the inter-dendritic eutectic regions during solidification.

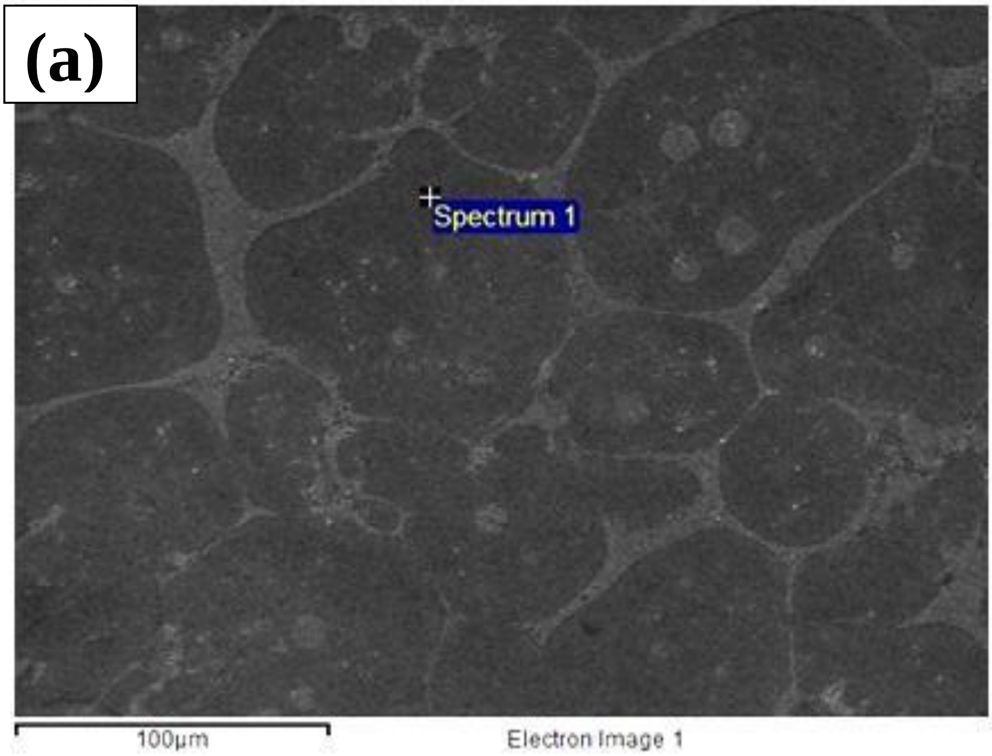

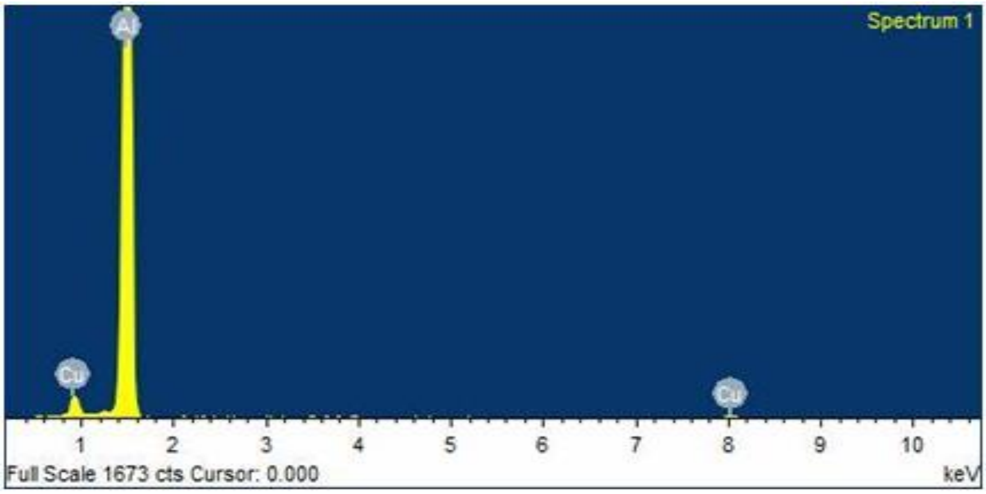

Element	Weight%	Atomic%
Al K	94.88	97.76
Cu K	5.12	2.24
Totals	100.00	

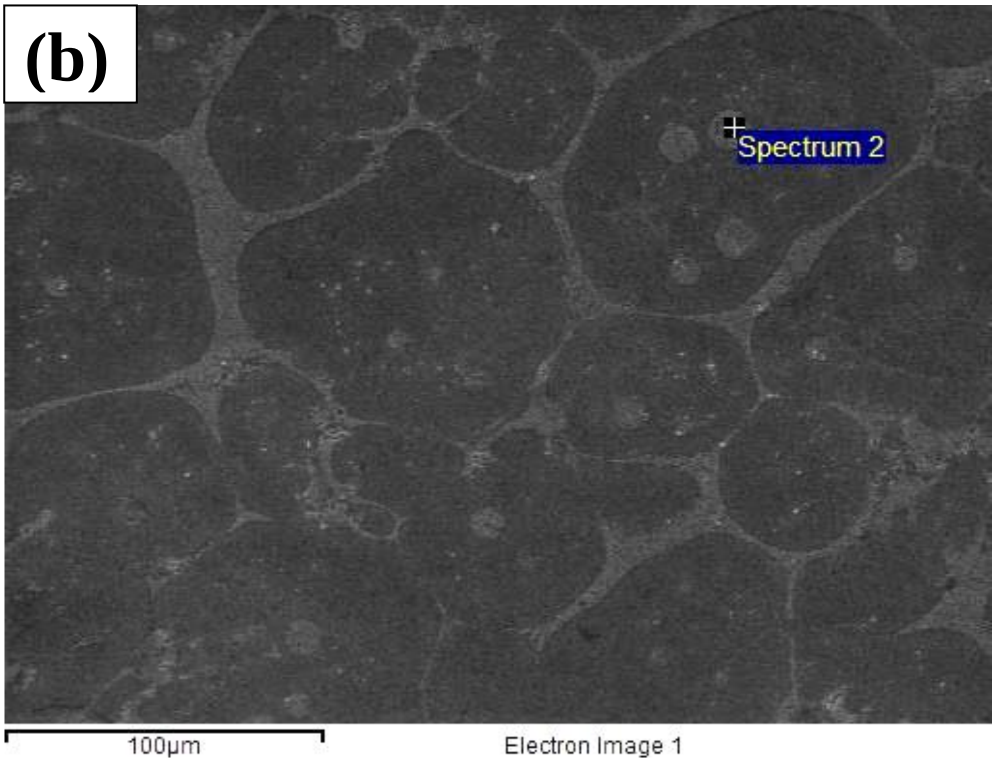

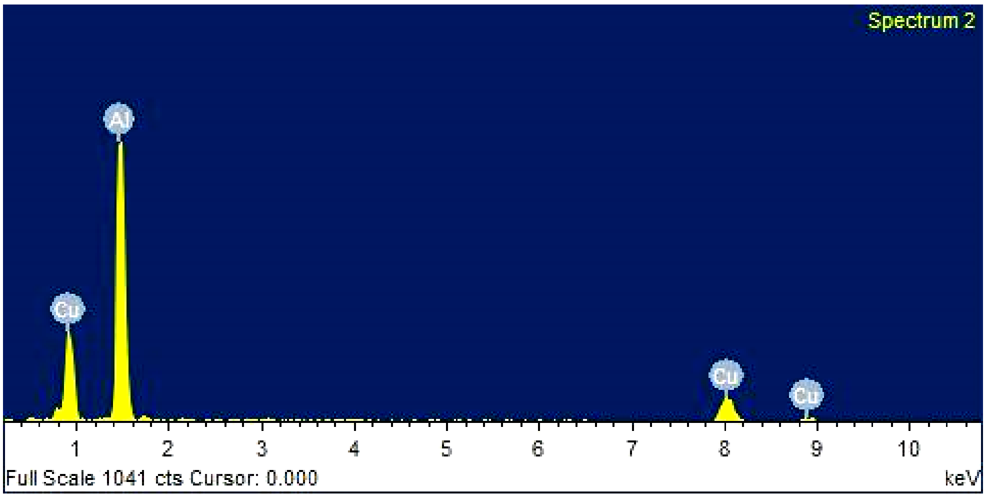

Element	Weight%	Atomic%
Al K	64.20	80.85
Cu K	35.80	19.15
Totals	100.00	

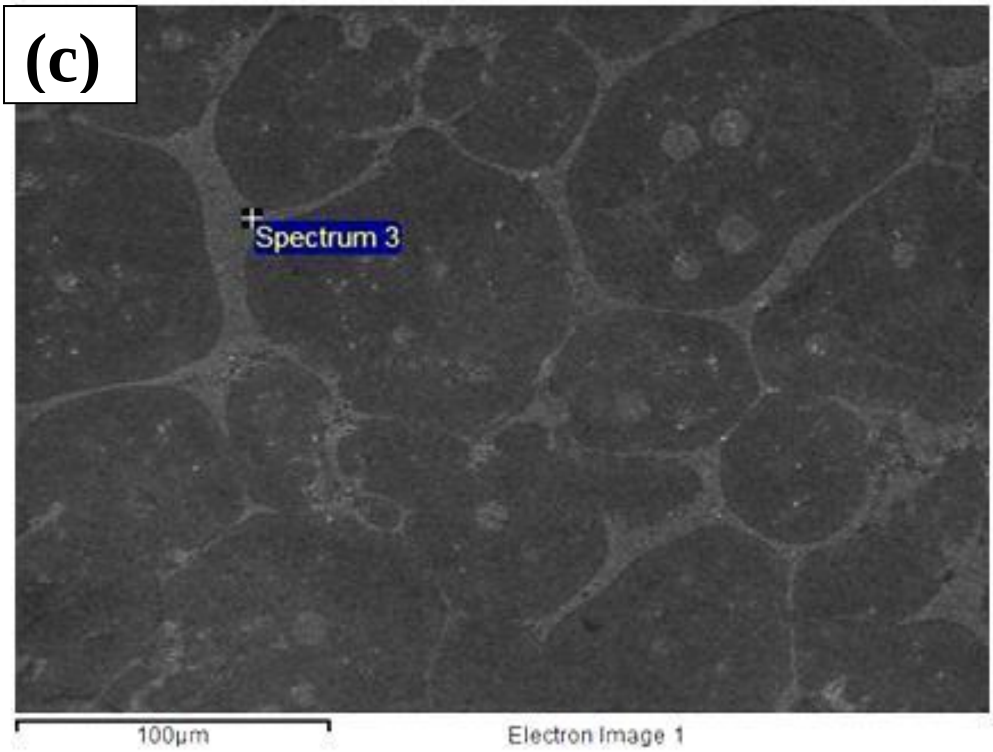

.

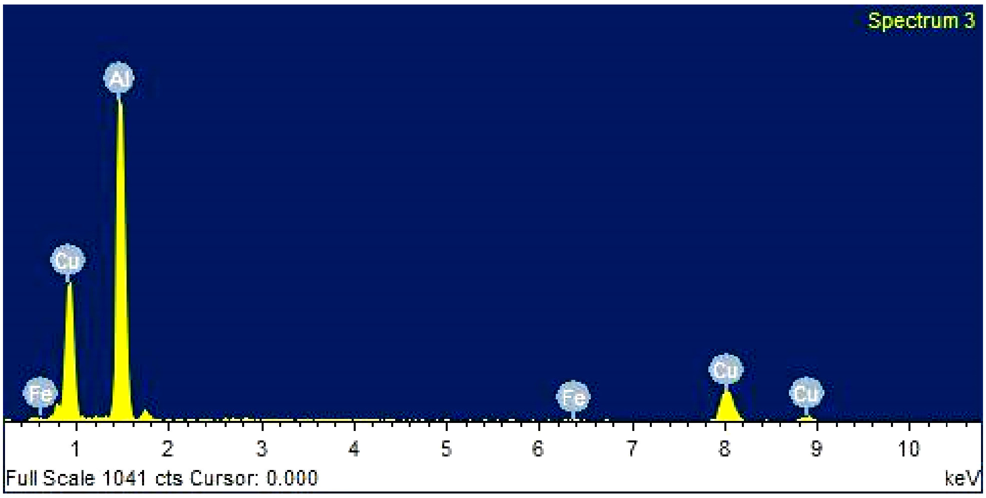

Element	Weight%	Atomic%
Al K	61.39	78.88
Fe K	0.74	0.46
Cu K	37.87	20.66
Totals	100.00	

Figure 4.9: EDS analysis results of stirred MMC upon 50% pre-deformation followed by heating at 580 °C for 30 minutes (*a*) matrix, (*b*) eutectic globular droplet and (*c*) grain boundary.

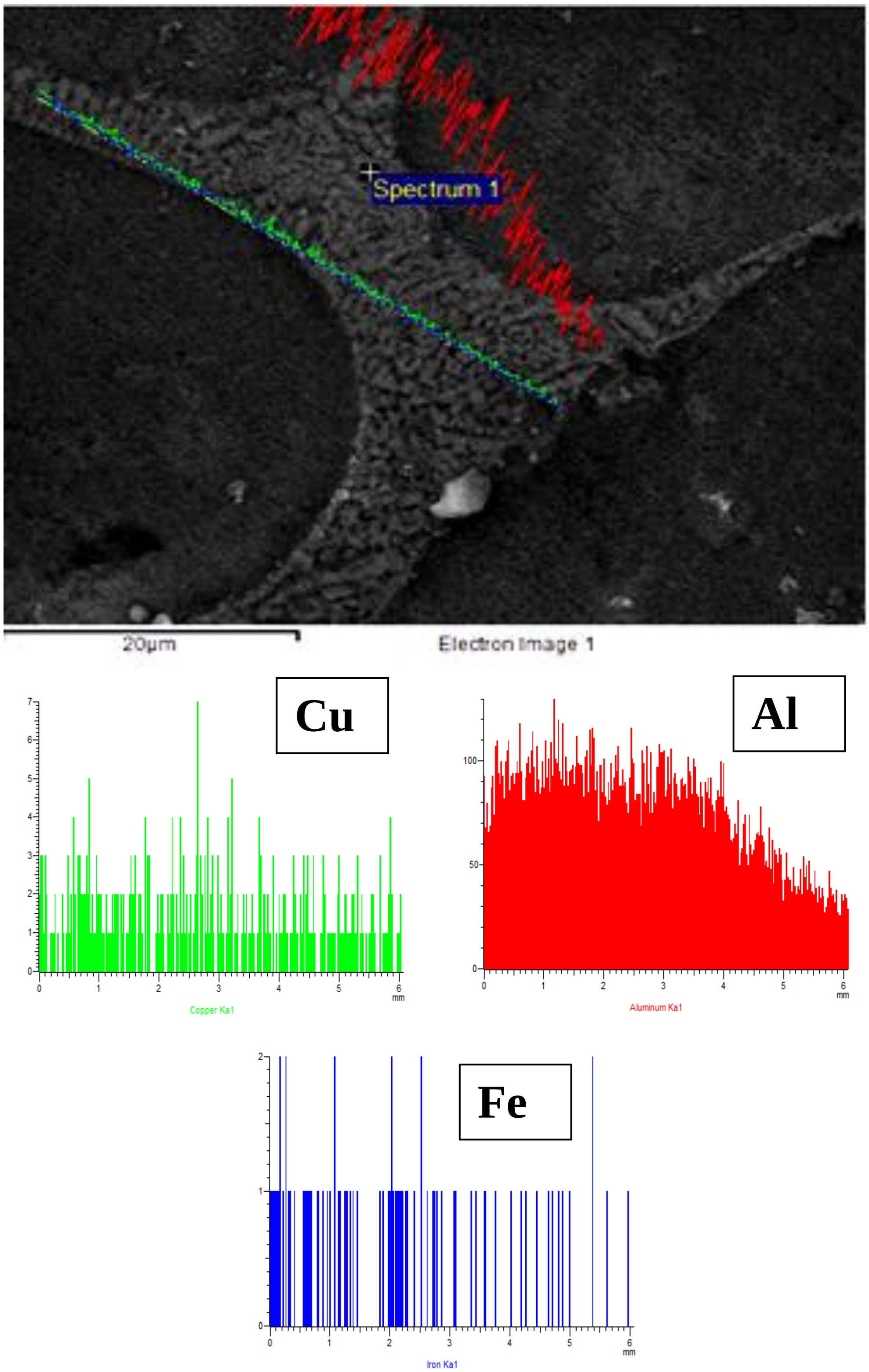

Figure 4.10: Results from line analysis in SIMA processed stirred MMC at eutectic grain boundary.

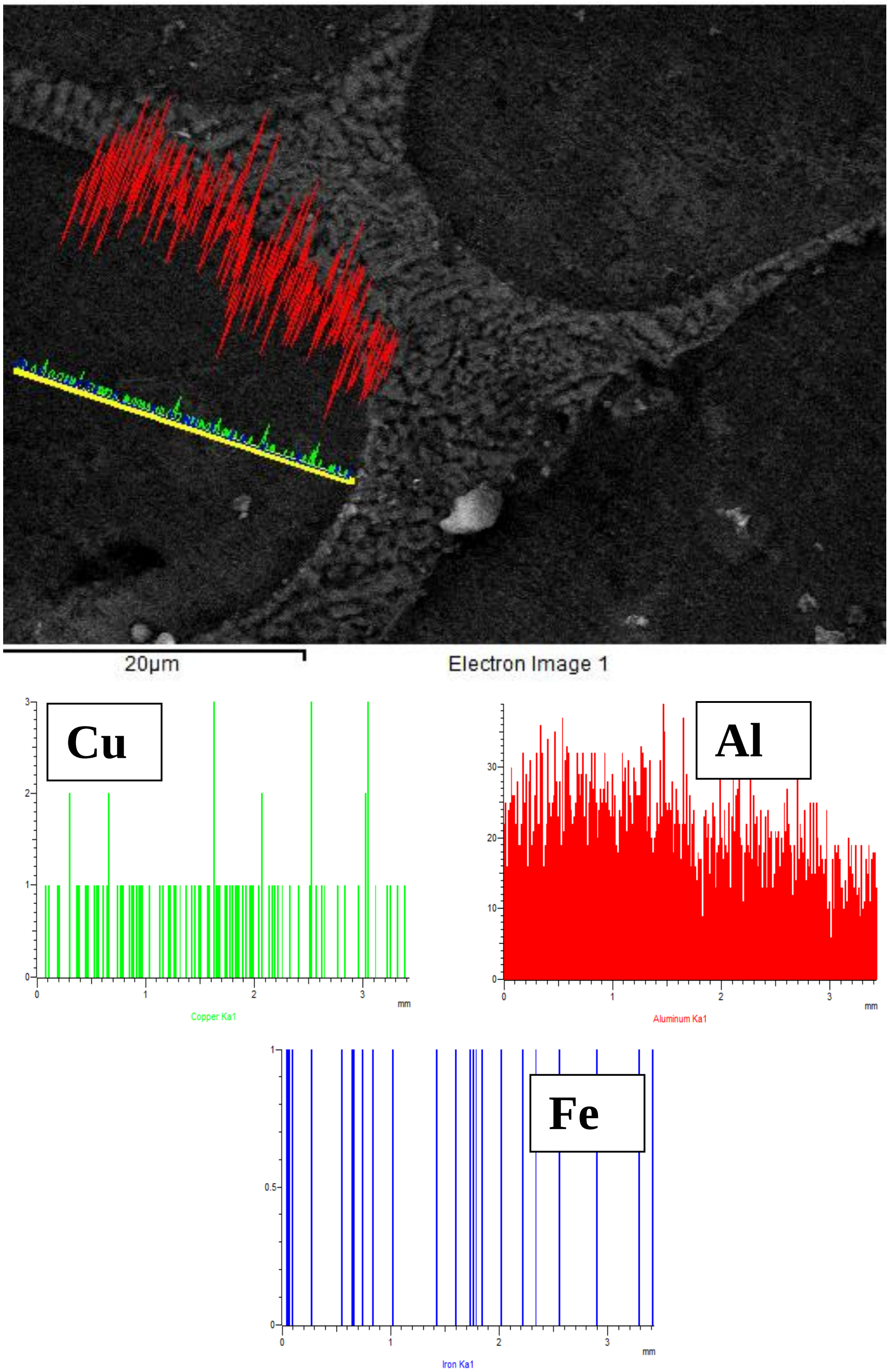

Figure 4.11: Results from line analysis in SIMA processed stirred MMC at primary phase matrix.

4.3.2. Mechanical Properties

In the Figure 4.12, MMC to SIMA indicates that metal mould casting subjected to SIMA process and SC to SIMA represents that stirred MMC subjected to SIMA process. Figure 4.12a shows the tensile strength of the MMC, stirred MMC subjected to SIMA process. Stirred MMC subjected to SIMA achieved good strength (230 MPa) compared to the MMC and MMC subjected to SIMA. Figure 4.12b compares the hardness of the alloy produced by the three routes, namely, MMC, stirred MMC subjected to 50 % pre-deformed SIMA alloy. Samples collected from the above processing methods were polished before evaluating hardness and average value of five readings has been reported. Clearly, the SIMA alloy has the highest hardness (156 HV), while the MMC shows the least hardness (96 HV) among the three samples. The low hardness of the MMC is due to progressive solidification leading to dendritic microstructure, while the high hardness of the SIMA processed samples may be related to a reduction in average grain size.

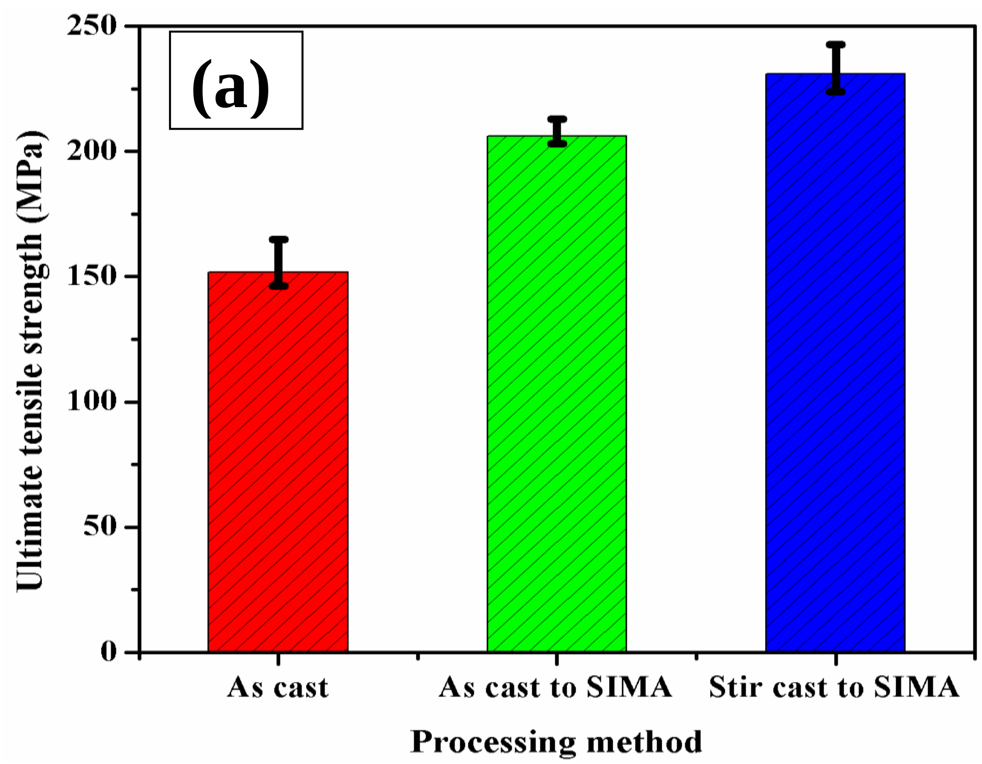

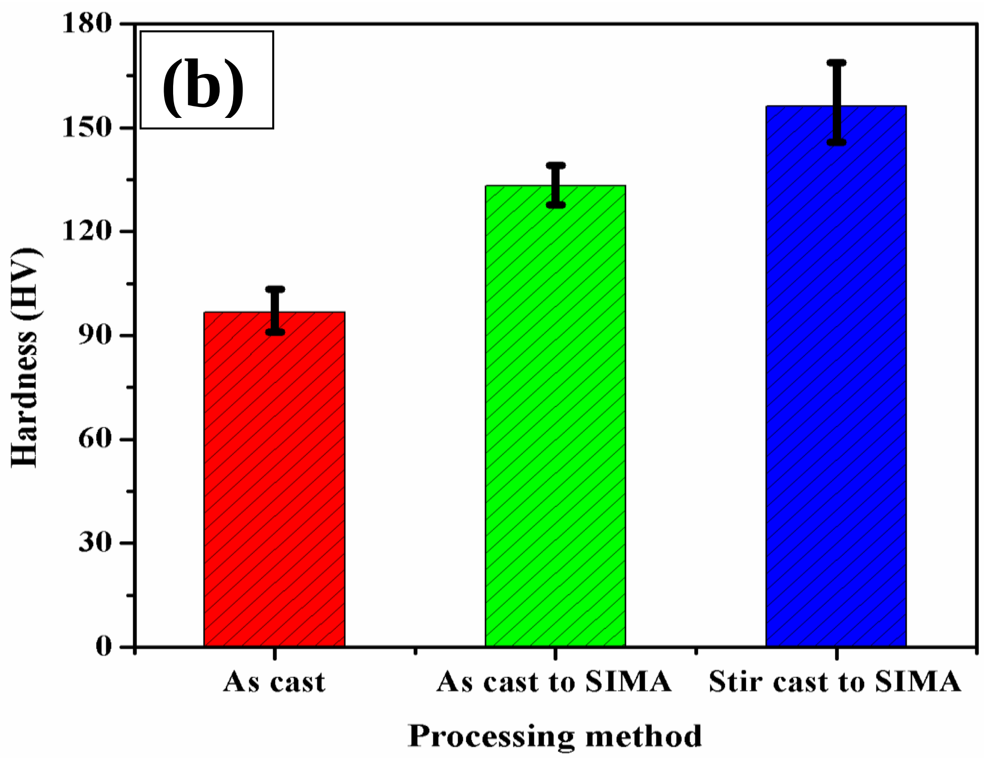

Figure 4.12: Graphs of Al-10Cu alloy (a) ultimate tensile strength *vs.* processing method, (*b*) hardness *vs.* processing method.

The fractured surfaces of the tensile tested samples for MMC, MMC subjected to SIMA and stirred MMC subjected to SIMA are shown in the Figure 4.13. Dimples along with some feature of cleavage fracture may be seen in all conditions. However, the tendency of cleavage fracture is more in MMC and fracture surface shows porosity and cracks which adversely affect the mechanical properties of the alloy. It may be clearly seen from the fractrographs (Figure 4.13b and 4.13c that the density of the shallow and fine dimples are higher in the samples MMC subjected to SIMA and stirred MMC subjected to SIMA.

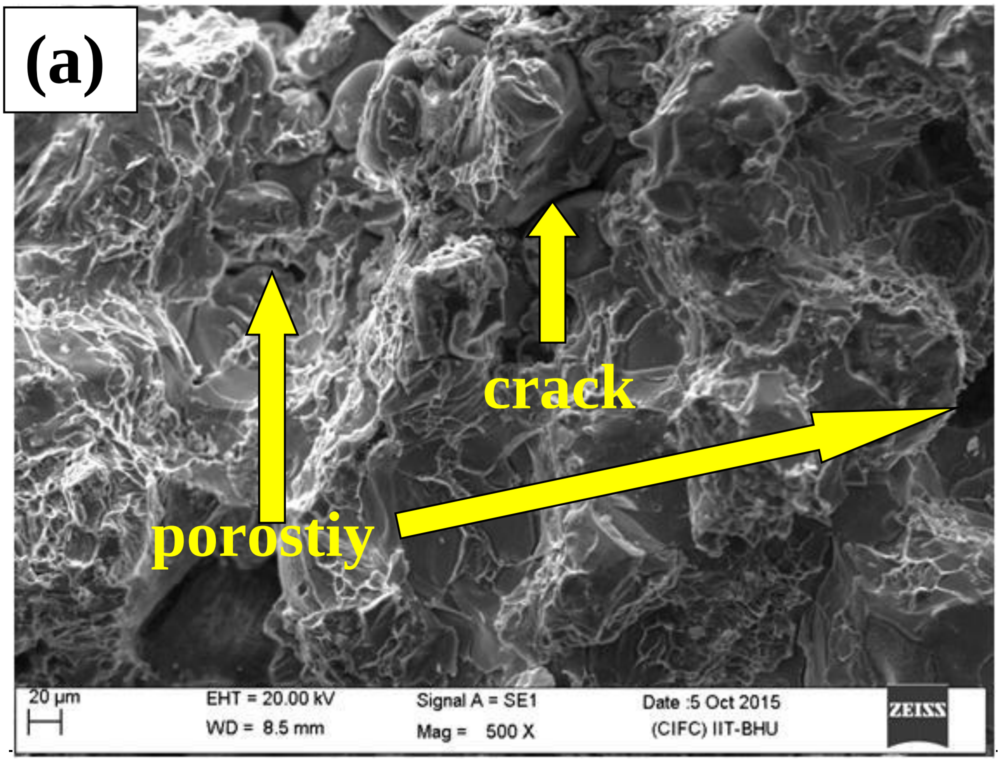
(a)
crack
porostiy
20 µm
EHT = 20.00 kV
WD = 8.5 mm
Signal A = SE1
Mag = 500 X
Date :5 Oct 2015
(CIFC) IIT-BHU
ZEISS

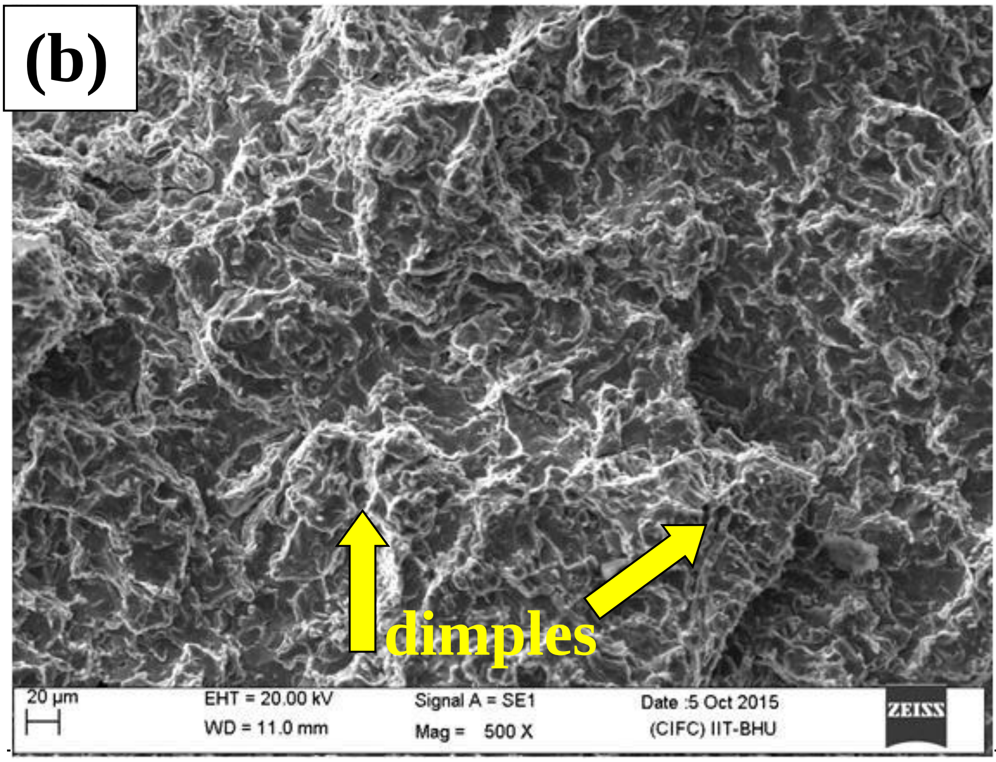
(b)
dimples
20 µm
EHT = 20.00 kV
WD = 11.0 mm
Signal A = SE1
Mag = 500 X
Date :5 Oct 2015
(CIFC) IIT-BHU
ZEISS

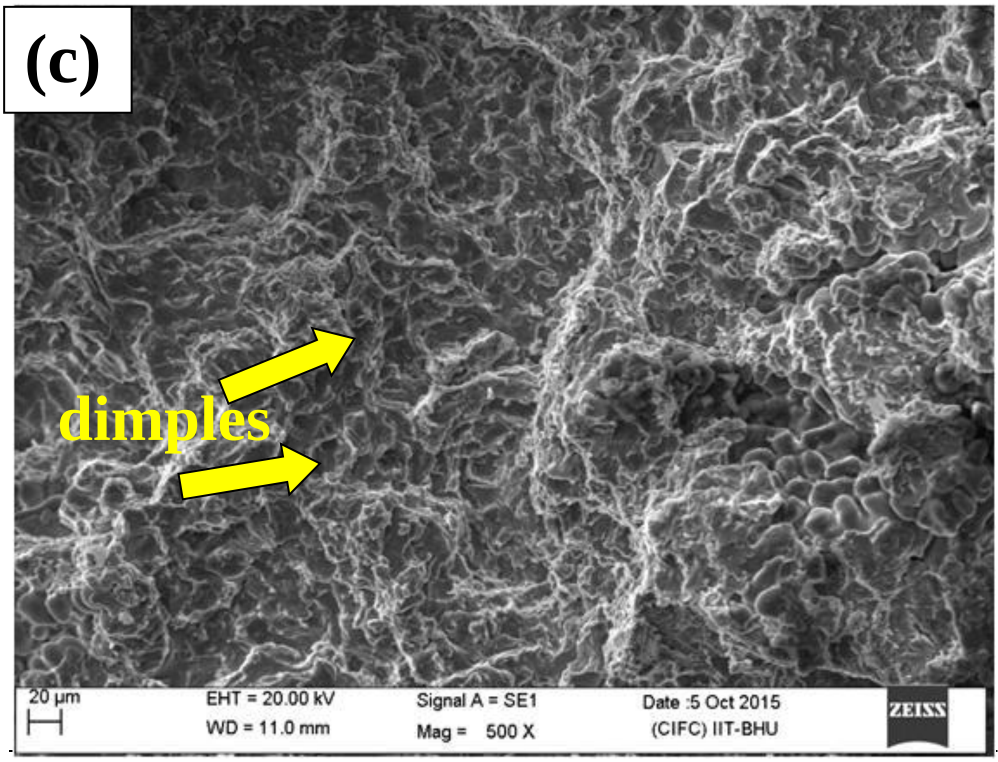

Figure 4.13: The SEM microstructures of a fractured surface of tensile specimens (*a*) MMC (*b*) MMC subjected to SIMA and (*c*) stirred MMC subjected to SIMA.

4.3.3 Wear Characteristics of Alloy

As shown by Archard[Archard, 1953] , wear volume of a material is a function of hardness and pressure. It is expressed by Archard's wear equation

$$Q = \frac{K * W}{H}$$

where Q = volume removed from the surface by wear per unit sliding distance, H = indentation hardness of the softer surface and W= normal pressure applied between the surface. The K is Archard's wear coefficient, which is dimensionless and always less than unity. The value of K helps in comparing the severity of different wear process. Gautam et al.[Gautam and Mohan, 2016] showed that the factors affecting the wear and friction behavior of materials are morphology, surface conditions prior to test and operating parameters.

The wear characteristics of Al-10Cu alloy produced by MMC and stirred MMC subjected to SIMA are investigated for different applied loads ranging from 10 to 40 N. The resistance to wear is quantified in terms of cumulative volume loss (CVL) during wear tests conducted at a constant sliding velocity of 1 m/s. The CVL is then determined for every 600 m intervals over a total sliding distance of 3600 m and is plotted in Figure 4.14. While the CVL of all processing methods increases with increasing sliding distance for any applied load as expected, a higher load also leads to enhanced material wear as can be seen from Figure 4.14. Among the three processing routes, the conventional MMC shows the highest wear for any applied load, while the stirred MMC subjected to SIMA exhibits the least wear. It is known that the sliding wear resistance of alloys critically depends on the microstructural features such as morphology, size and distribution intermetallic phases.[Wang et. Al., 2001] The small grain size, resulting in higher volume of the α-phase at the grain boundaries in the stirred MMC subjected to SIMA process is thus believed to be responsible for its improved wear resistance. The wear rate of the stirred MMC subjected to SIMA is less compared to MMC and MMC subjected to SIMA. The wear rate of the MMC had rapidly increased beyond 1800 m sliding distance compared to the MMC and stirred MMC subjected to SIMA. Figure 4.15a indicates the variation in the wear rate of the MMC, MMC and stirred MMC subjected to SIMA with the applied load. The wear rate of stirred MMC subjected to SIMA is low as compared to the MMC and MMC subjected to SIMA. The better wear rate of SIMA processed sample is due to the globular morphology of the primary α grains and lowest average grain size.

The coefficient of friction was calculated by dividing the frictional force with the corresponding applied loads. The variation in the coefficient of friction of MMC, stirred MMC subjected to SIMA is plotted in Figure 4.15b as a function of sliding distance at a constant sliding velocity of 1 m/s and constant load 40 N. The coefficient of friction of stirred MMC subjected to SIMA can be seen to have decreased with increasing in sliding distance and which is lower as compared to MMC and MMC subjected to SIMA. Coefficient of friction is higher at the lower load and decreased with increasing in load which is consistent with previous report.[Anasyida et al. 2010] Van et al.[Thuong et. Al., 2015] suggested that the true contact of the full surface was not created because of asperity locking increased the coefficient friction at low load. Dwivedi et al.[Dwivedi et. Al., 2004] reported that the coefficient of friction depends on the material properties like hardness, ultimate tensile strength. The coefficient of friction has decreased to a low value at higher load because of decreased shear strength. This is due to higher applied force to increase the interface temperature between the contact surfaces and formed the very fine molten layer at the asperities interactions. The low friction of the stirred MMC subjected to SIMA induces the lowest wear rate, which was agreed with earlier report [Vencl et. Al., 2014].

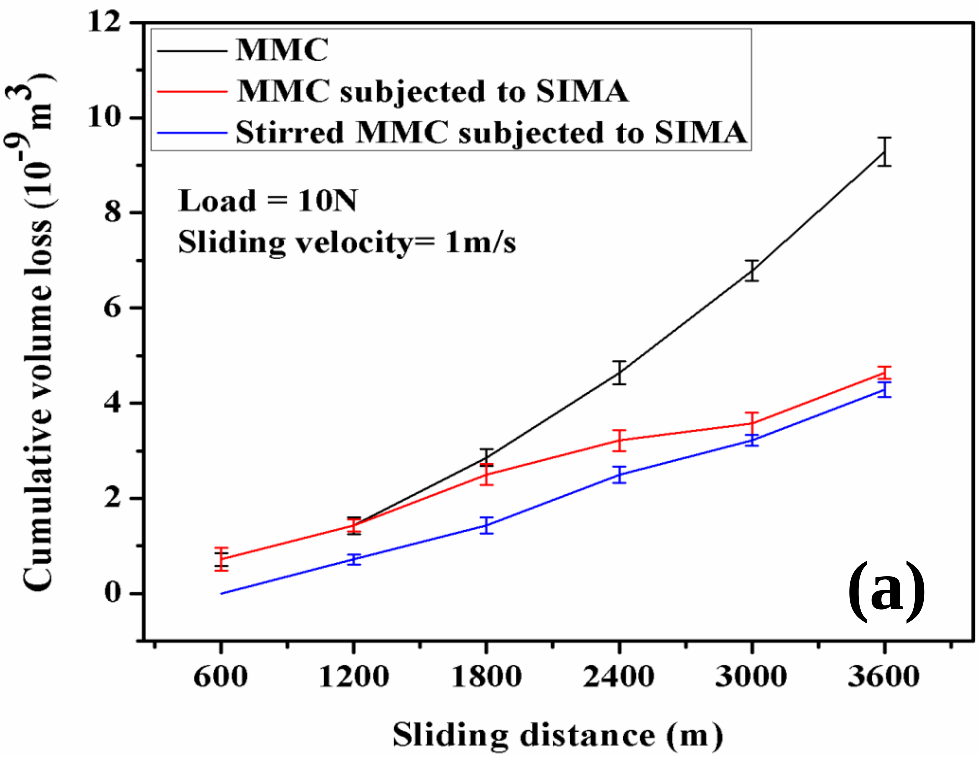

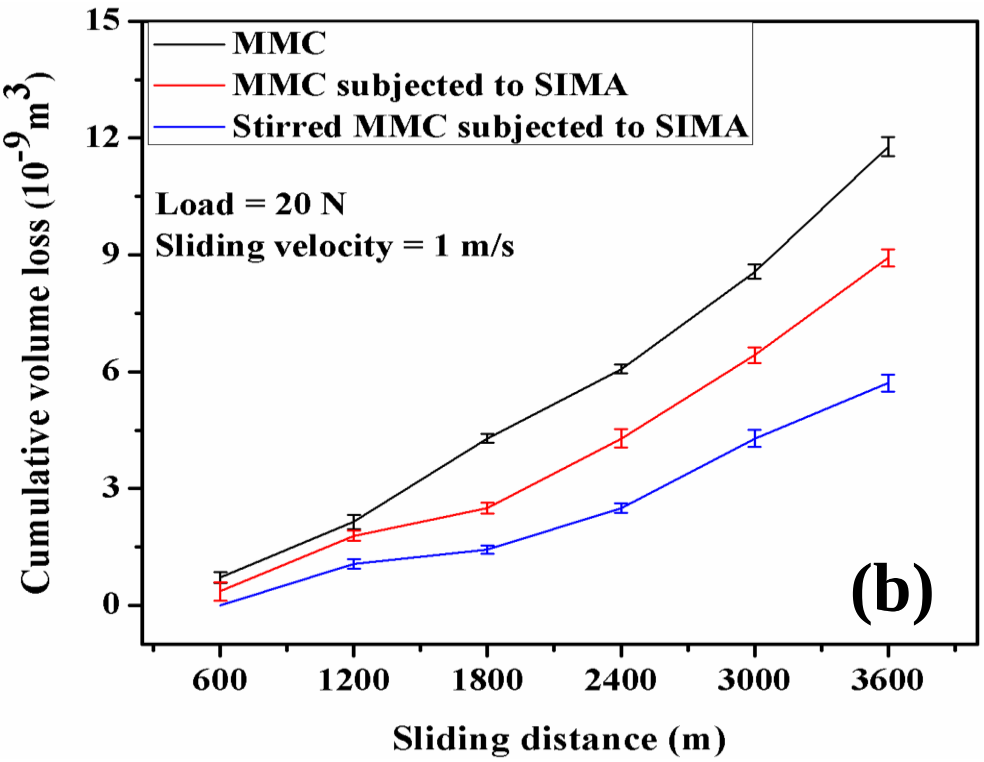
MMC
MMC subjected to SIMA
Stirred MMC subjected to SIMA
Load = 20 N
Sliding velocity = 1 m/s
(b)
Cumulative volume loss (10^{-9} m^3)
Sliding distance (m)
0
3
6
9
12
15
600
1200
1800
2400
3000
3600

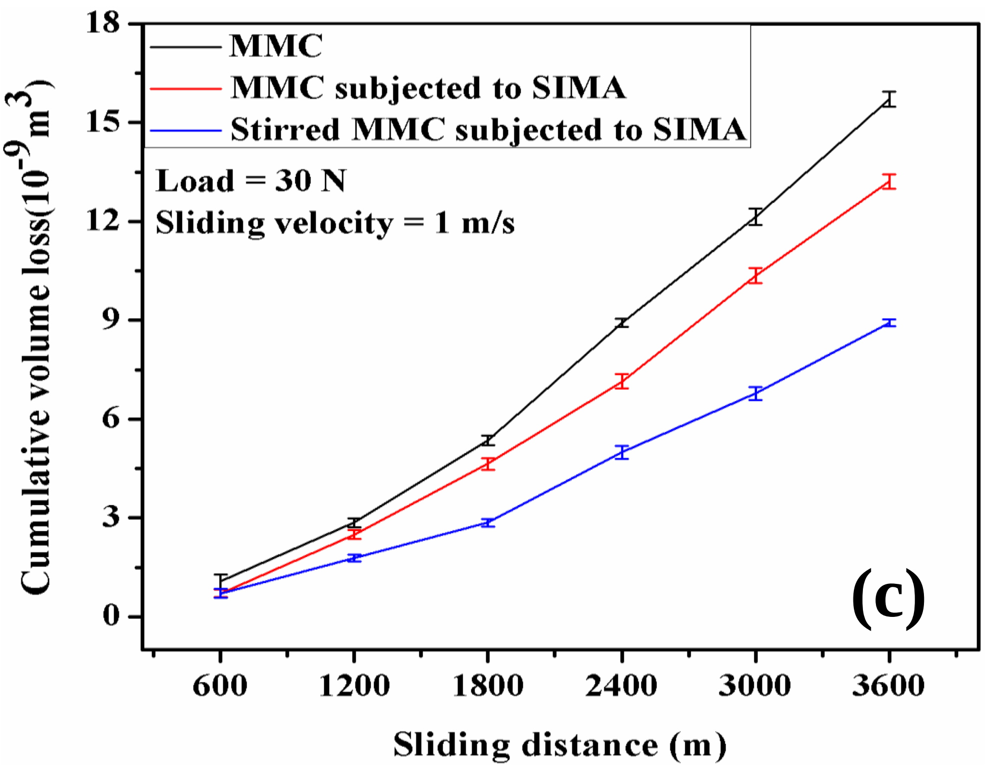
MMC
MMC subjected to SIMA
Stirred MMC subjected to SIMA
Load = 30 N
Sliding velocity = 1 m/s
(c)
Cumulative volume loss(10^{-9} m^3)
Sliding distance (m)
0
3
6
9
12
15
18
600
1200
1800
2400
3000
3600

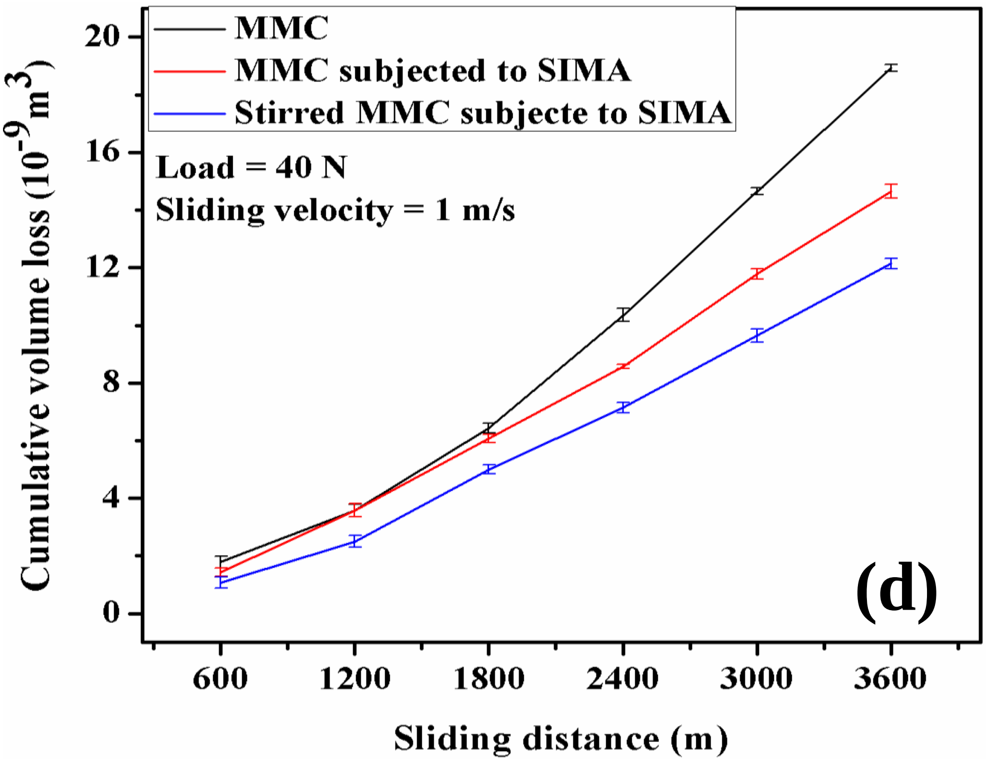

Figure 4.14: Variation of cumulative volume loss with sliding distance MMC, MMC subjected to SIMA and stirred MMC subjected to SIMA at (*a*) 10N, (*b*) 20 N, (*c*) 30 N, and (*d*) 40 N.

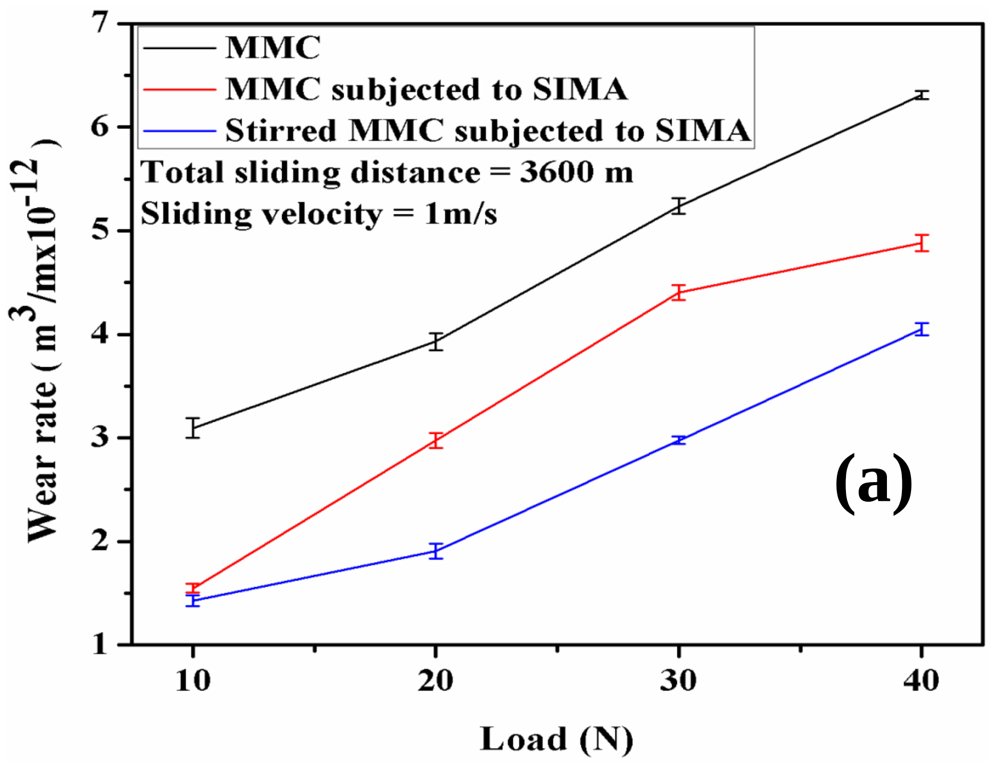

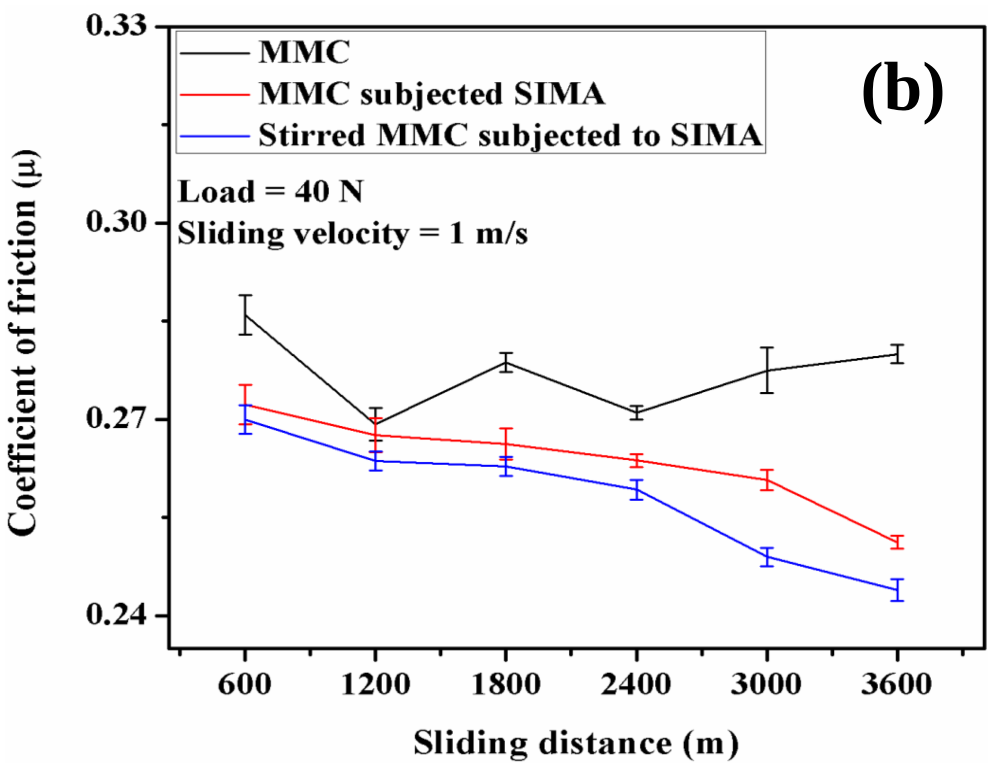

Figure 4.15: (*a*) variation of wear rate as a function of normal load, (*b*) variation of the coefficient of friction with sliding distance at 40 N of MMC, MMC subjected to SIMA and stirred MMC subjected to SIMA.

4.3.4 Morphology of worn-out surfaces

The worn surfaces of the wear pin samples were examined under SEM to investigate the wear mechanism. Figure 4.16a shows the morphologies of the worn surfaces of the metal mould casting of 40 N at a sliding velocity of 1 m/s for the total sliding distance of 3600 m. The micrograph contains longitudinal and transverse cracks along with severe damaged regions. This indicates the combination of adhesive and delamination mode of wear. The dendritic structure and porosity in the interdendritic regions of the MMC helped to nucleated the cracks. These cracks were interconnected and promoted the removal of material in the form of sheets and left craters finally. These cracks penetrations caused the delamination and adhesive wear in the MMC. The worn surface of the MMC subjected to the SIMA process at an applied load of 40N was found to have been less damaged as compared to the corresponding MMC shown in Figure 4.18a. The extent of wear in these samples was lower than that of the MMC. Small patches, abrasive scoring marks were observed. The worn surface of the Stirred MMC subjected to the SIMA process at a load of 40 N is characterized by fine grooves running from one end to the other end of the pin (Figure 4.19a). Abrasion marks along with oxides of worn surface show the abrasive wear mechanism. Dey et al. [Dey and Poddar, 2006] suggested that wear by abrasion or scoring may not result high wear loss since the amount of material removed from a fine groove is small. The wear rate of the material reduces with increasing hardness under the abrasive wear mechanism.[Alshmri et al. 2014, Nodooshan et al. 2014 and Alidokht et al.2012]. The wear behavior of a material can be predicted with the hardness, but again, it is constrained by its microstructure.[Vencl et al. 2010] The abrasive wear of the material is controlled by the hardness and its microstructure. The stirred MMC subjected to the SIMA process has less average grain size, good hardness and improved globular microstructure as compared to MMC and MMC subjected to SIMA process. The liquid droplets entrained in the grains have improved the wear behavior of the stirred MMC subjected to the SIMA process which was supported by the results of our previous work (chapter-2). Figures 4.16b, 17 and 18b and 19b show the contour of worn surfaces and different level of surface roughness, texture, waviness and 3D topography produced during wear testing of Metal mould casting (MMC), MMC and stirred MMC subjected to SIMA respectively. These profiles indicate the variation of surface roughness from valley to peak, which is also reported elsewhere.[Gautam et al. 2016] To see the nature of the profile of the particular area of the worn surface, an average line is drawn in contour which has shown the nature of profile on that particular line. 3D–profilometer image and line analysis results are confirming the results of the R_a value of the alloy casts. 3D profile of metal mold casting shows more roughness value compared to MMC and stirred MMC subjected to SIMA process. The surface roughness values of MMC, MMC subjected to SIMA and stirred MMC subjected to SIMA are 1.2, 0.9 and 0.5μm respectively. Dendritic microstructure changed into globular primary phase during the SIMA process and improved its hardness, ultimate tensile strength and wear properties which results in variation of the average roughness values.

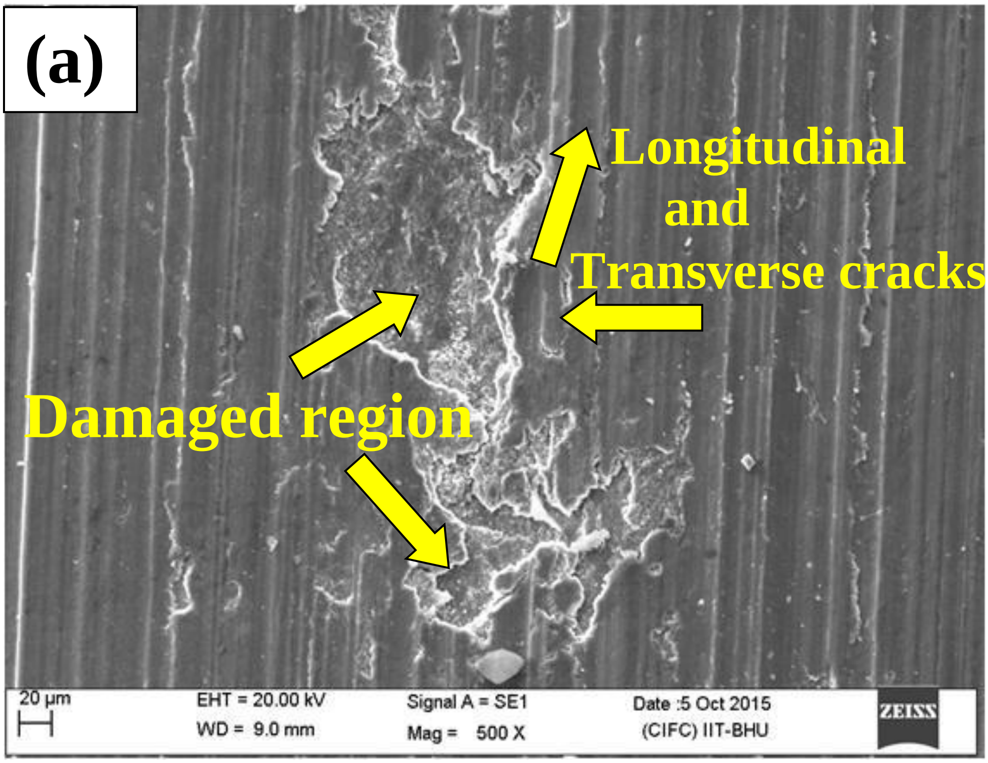

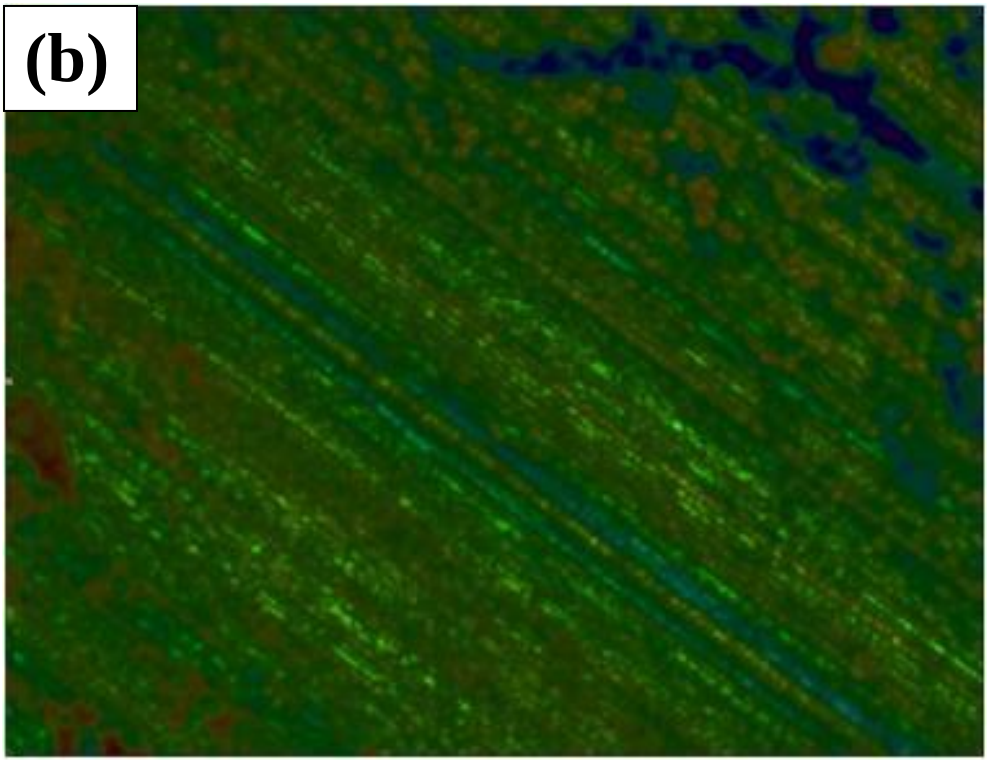

Figure 4.16: Worn surface topography of the Metal mould casting (MMC) at 40 N load and 1 m/s sliding velocity under SEM and profilometer.

.

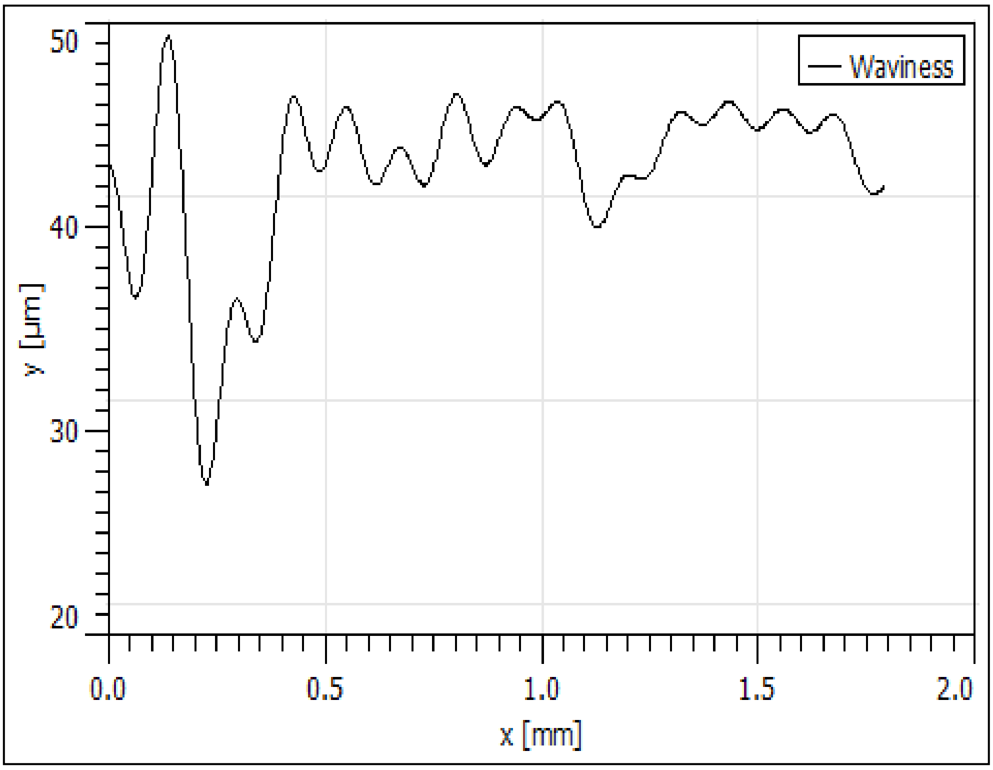

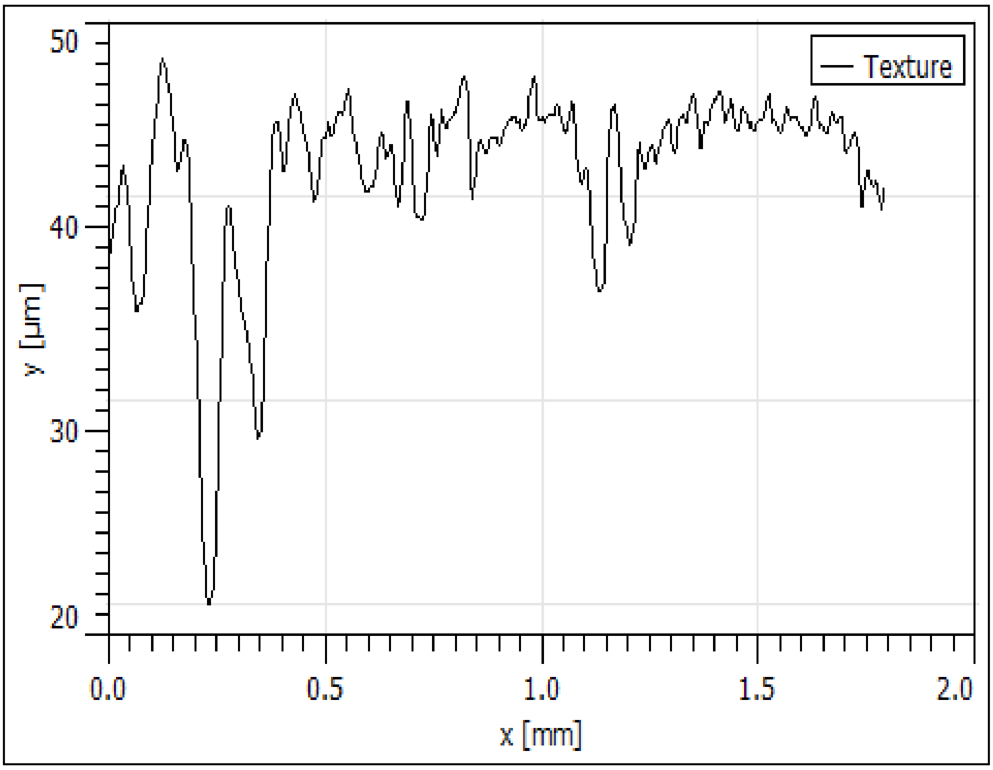
Texture
50
40
30
20
y [µm]
0.0
0.5
1.0
1.5
2.0
x [mm]

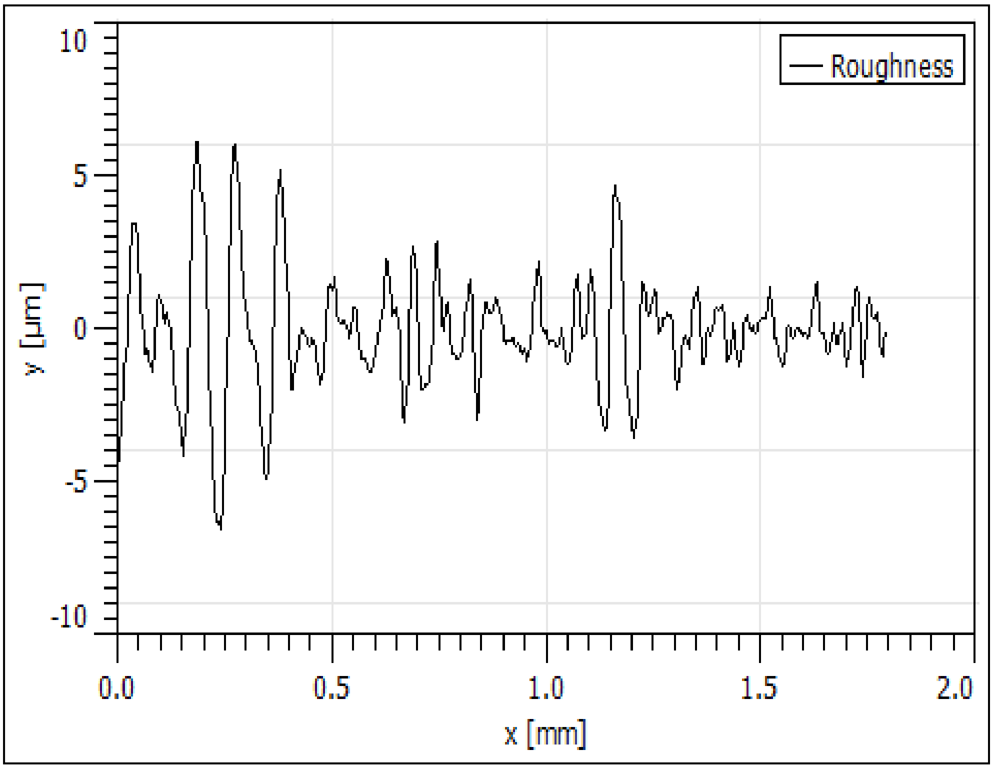
Roughness
10
5
0
-5
-10
y [µm]
0.0
0.5
1.0
1.5
2.0
x [mm]

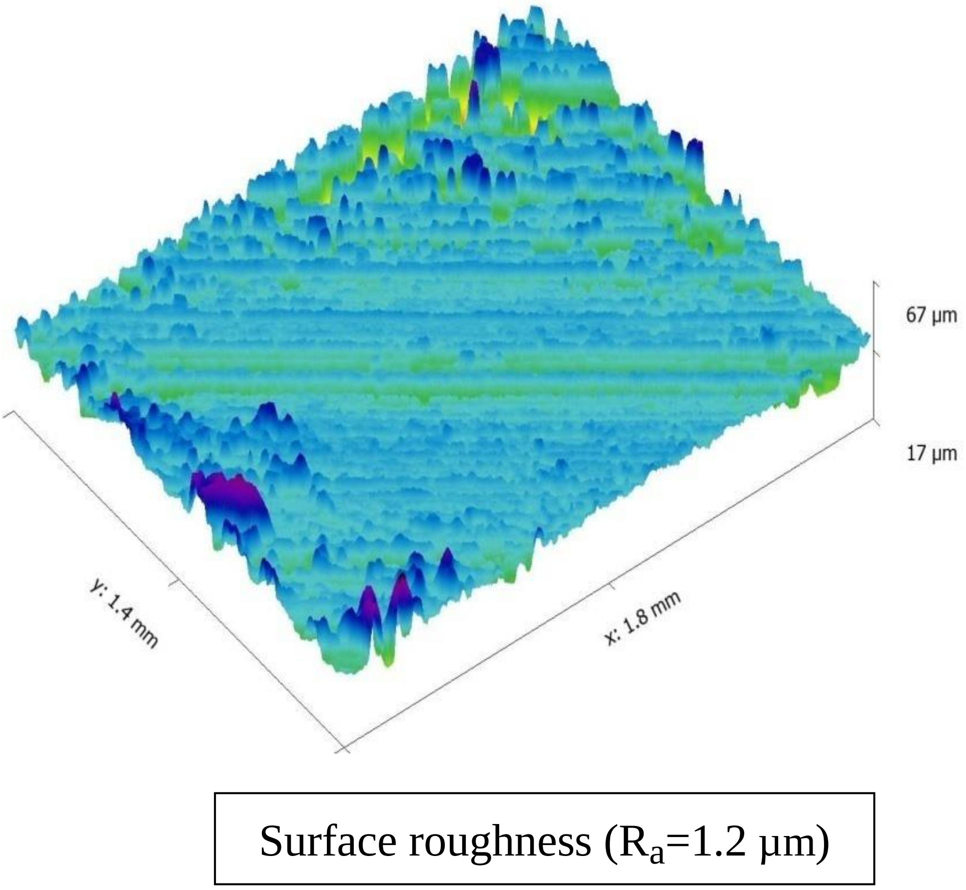

Figure 4.17: Worn surface topography of the Metal mould casting (MMC) at 40 N load and 1 m/s sliding velocity under SEM and profilometer.

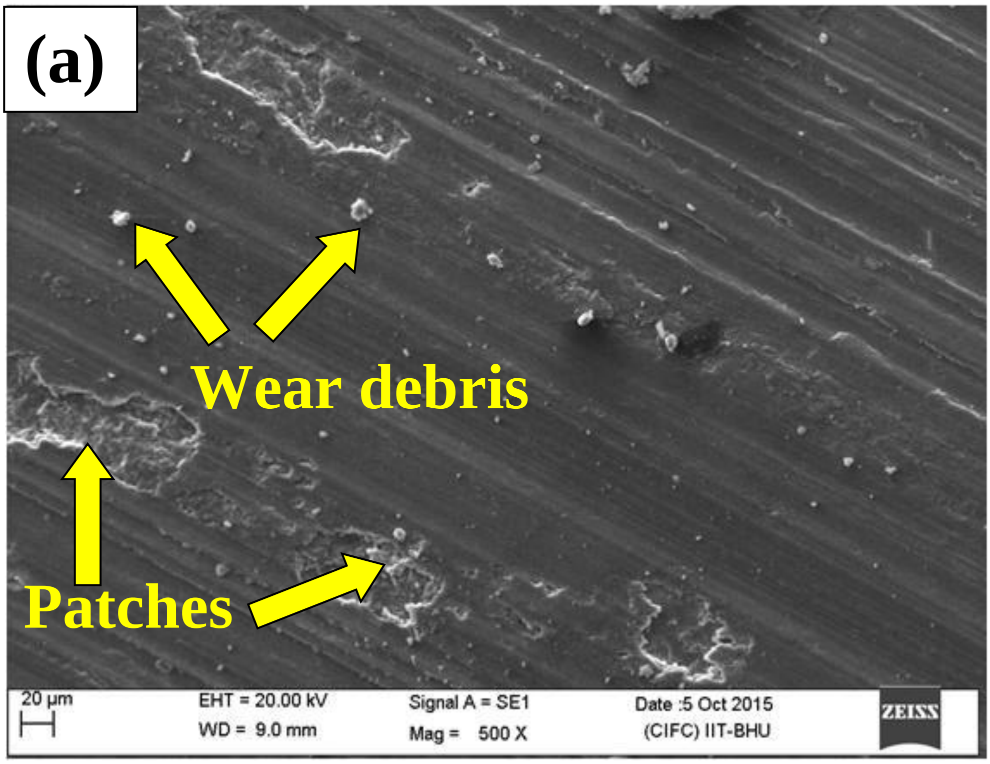

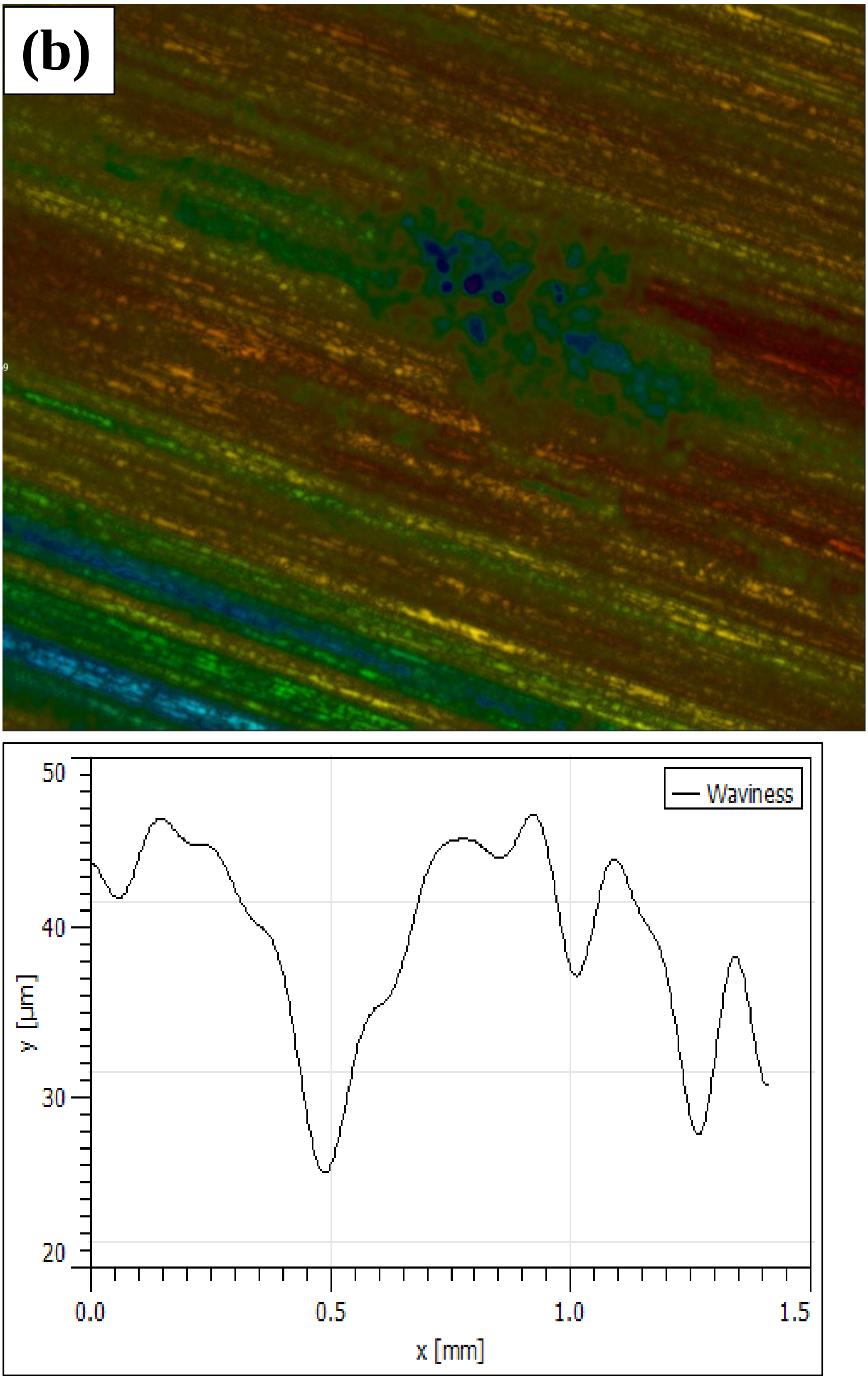
(b)
Waviness
50
40
30
20
y [µm]
0.0
0.5
1.0
1.5
x [mm]

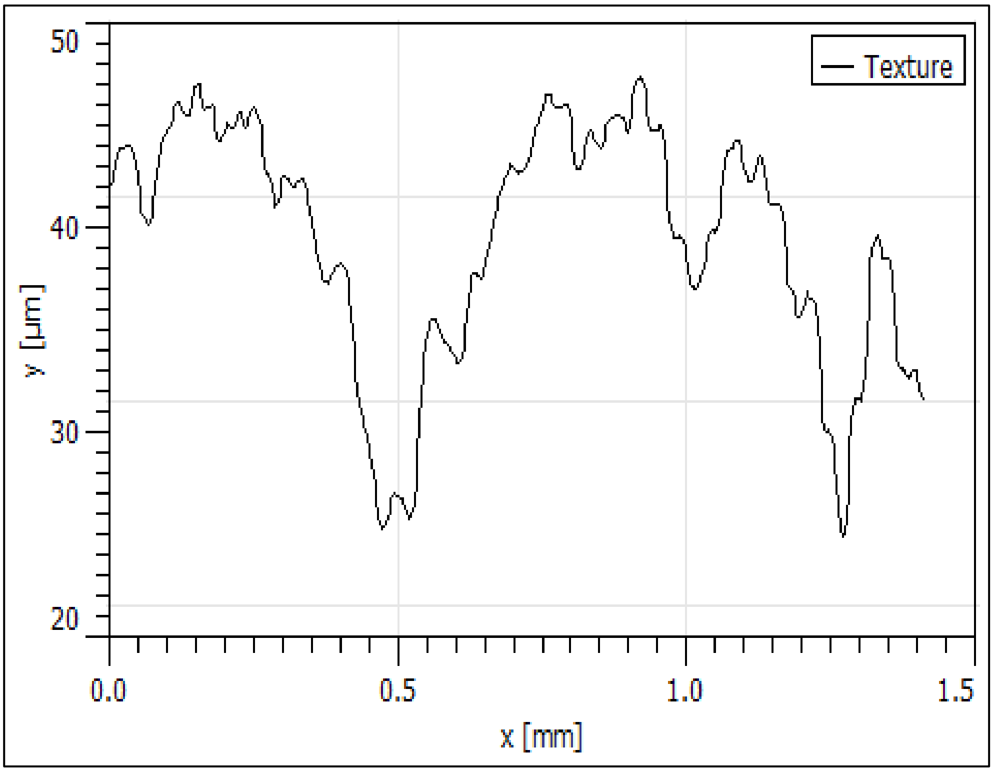
Texture
y [µm]
50
40
30
20
0.0
0.5
1.0
1.5
x [mm]

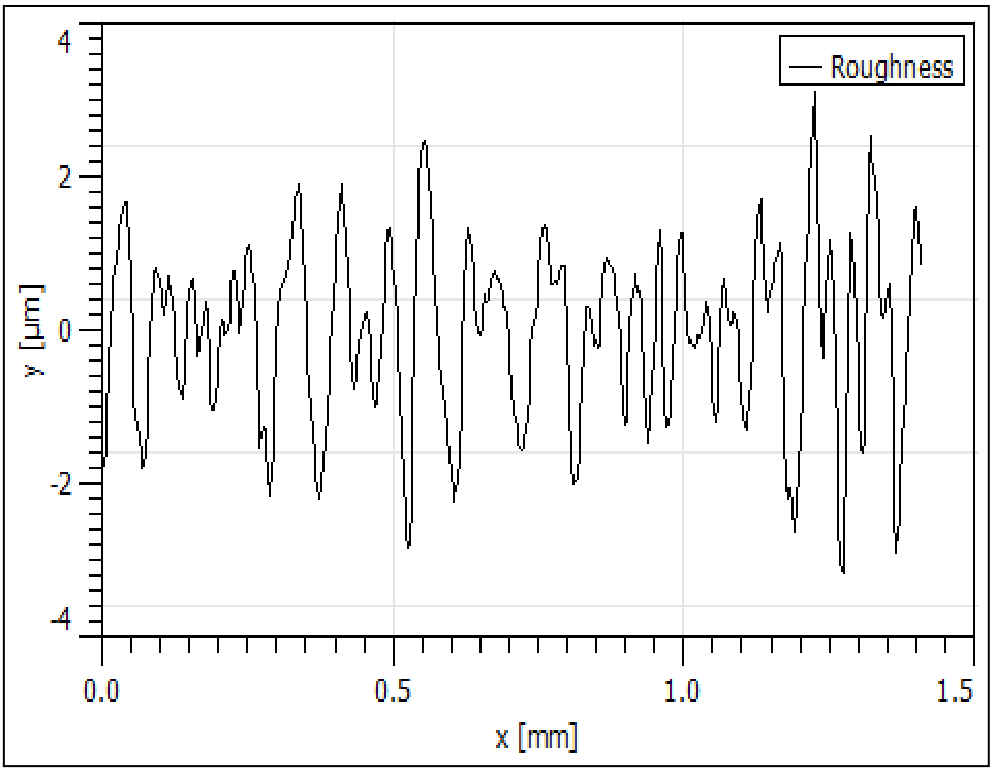
Roughness
y [µm]
4
2
0
-2
-4
0.0
0.5
1.0
1.5
x [mm]

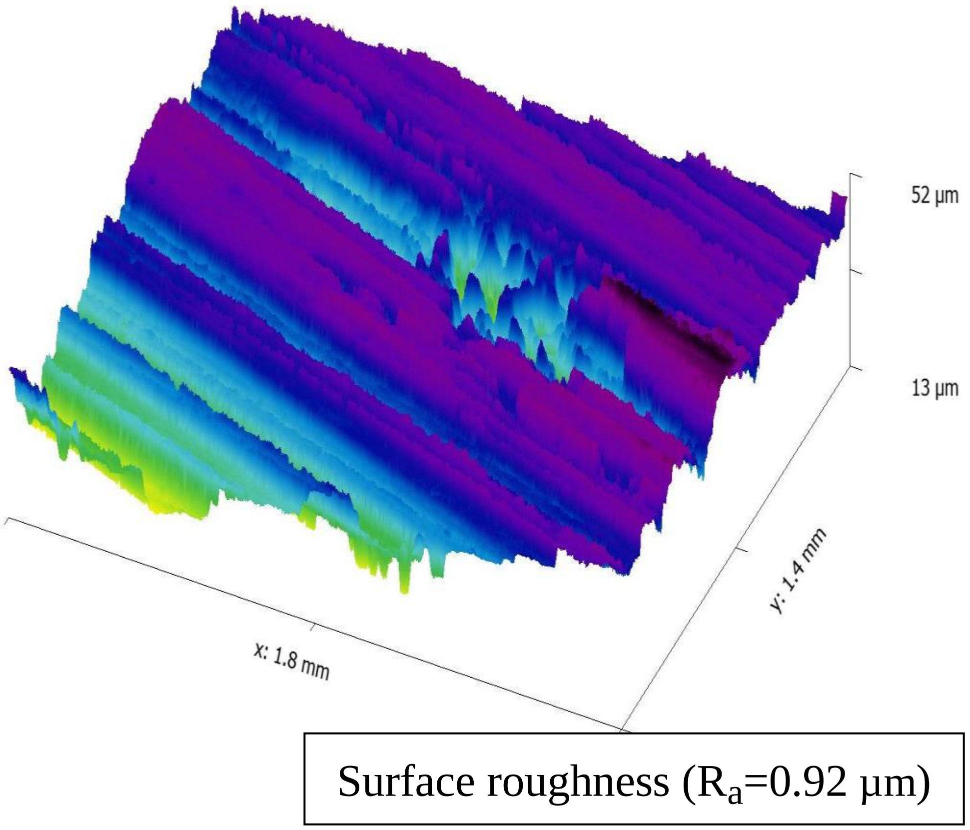

Figure 4.18: Worn surface topography of the MMC subjected to SIMA at 40 N load and 1 m/s sliding velocity under SEM and profilometer.

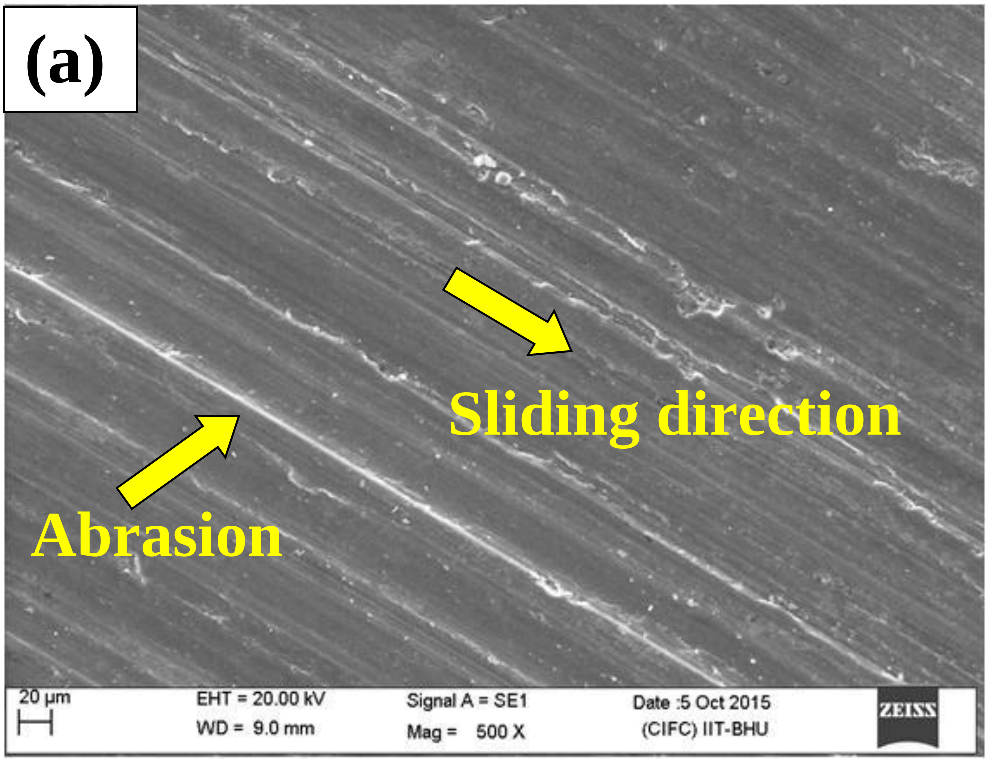

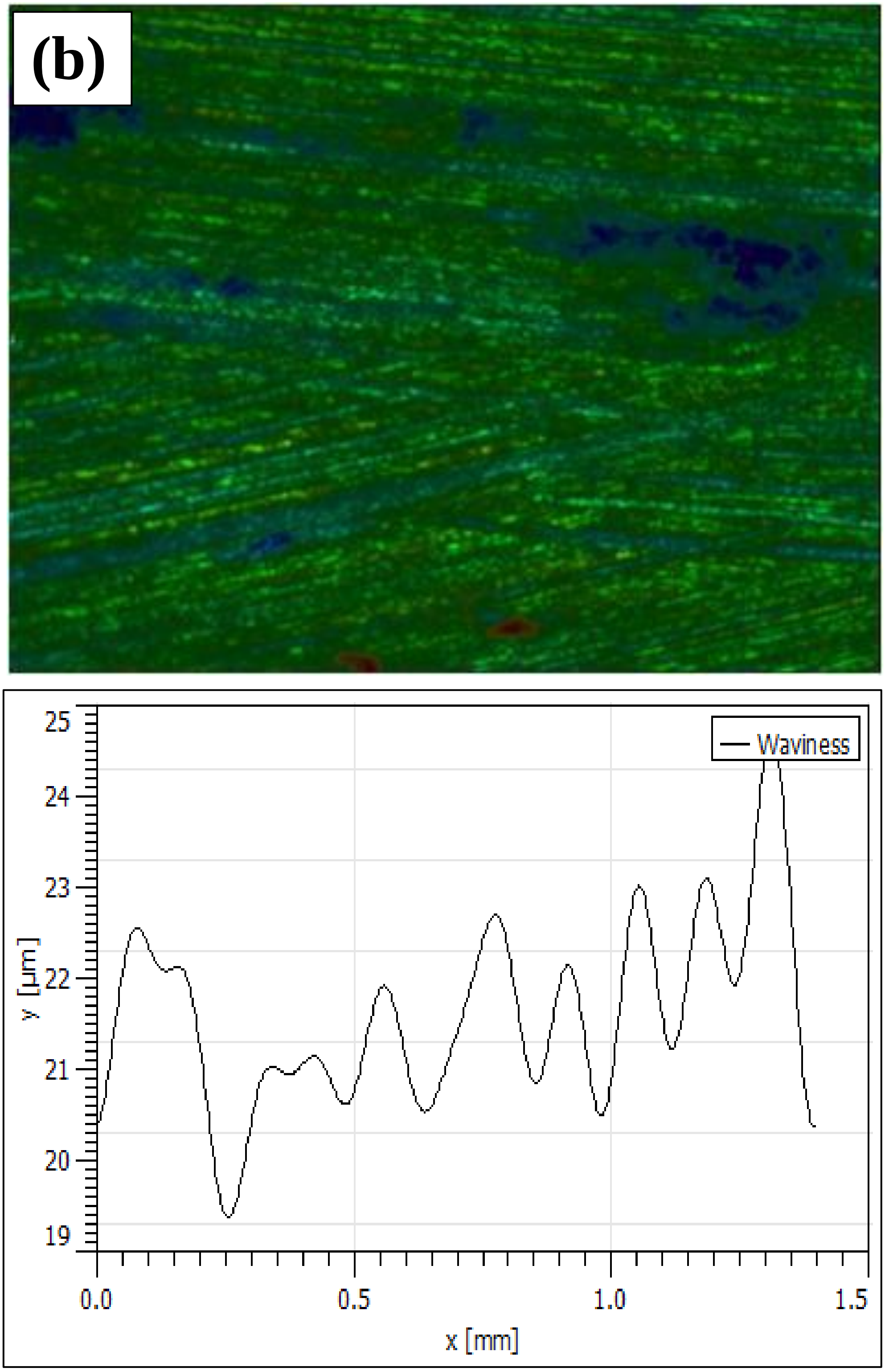
(b)
Waviness
y [µm]
x [mm]
19
20
21
22
23
24
25
0.0
0.5
1.0
1.5

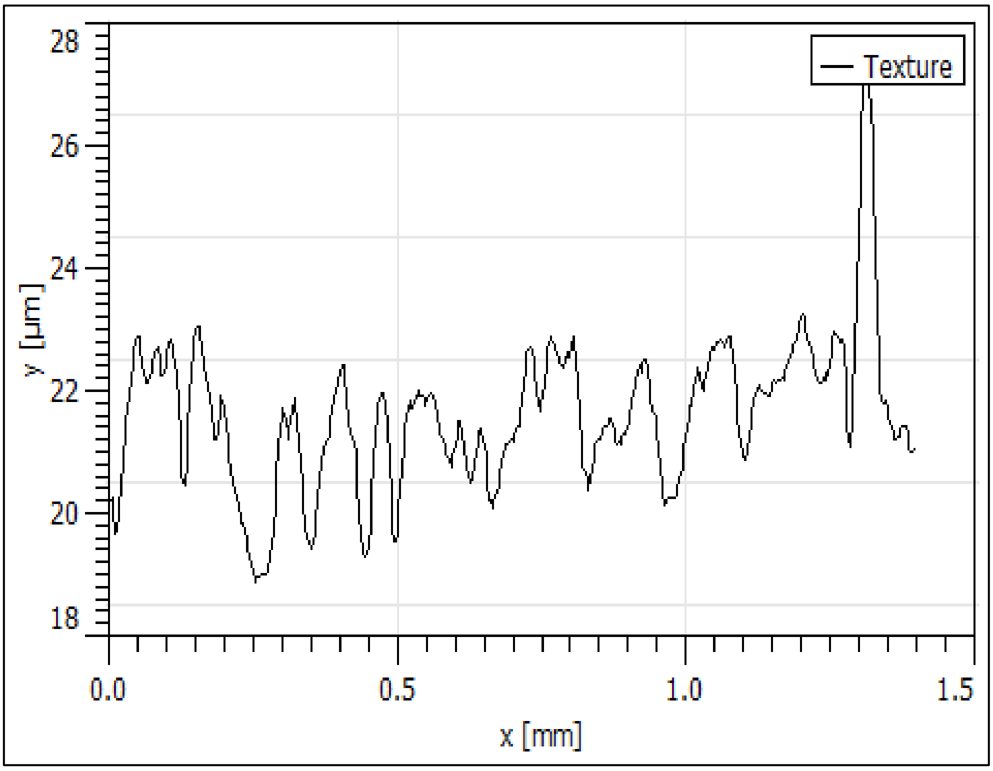
Texture
y [µm]
28
26
24
22
20
18
0.0
0.5
1.0
1.5
x [mm]

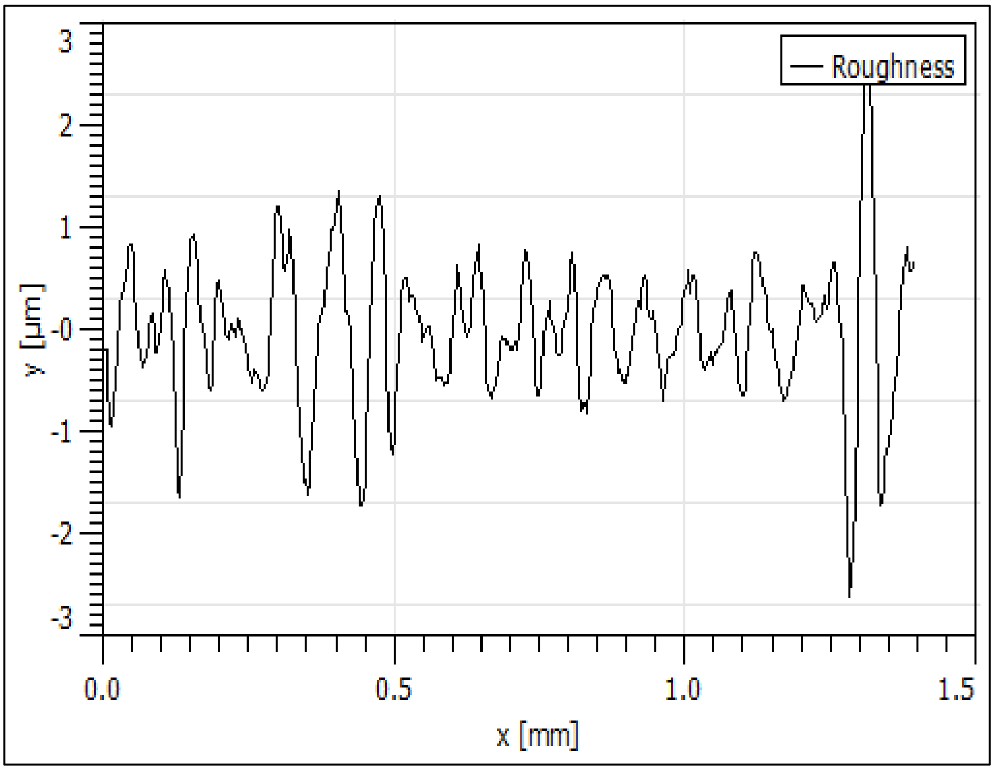
Roughness
y [µm]
3
2
1
-0
-1
-2
-3
0.0
0.5
1.0
1.5
x [mm]

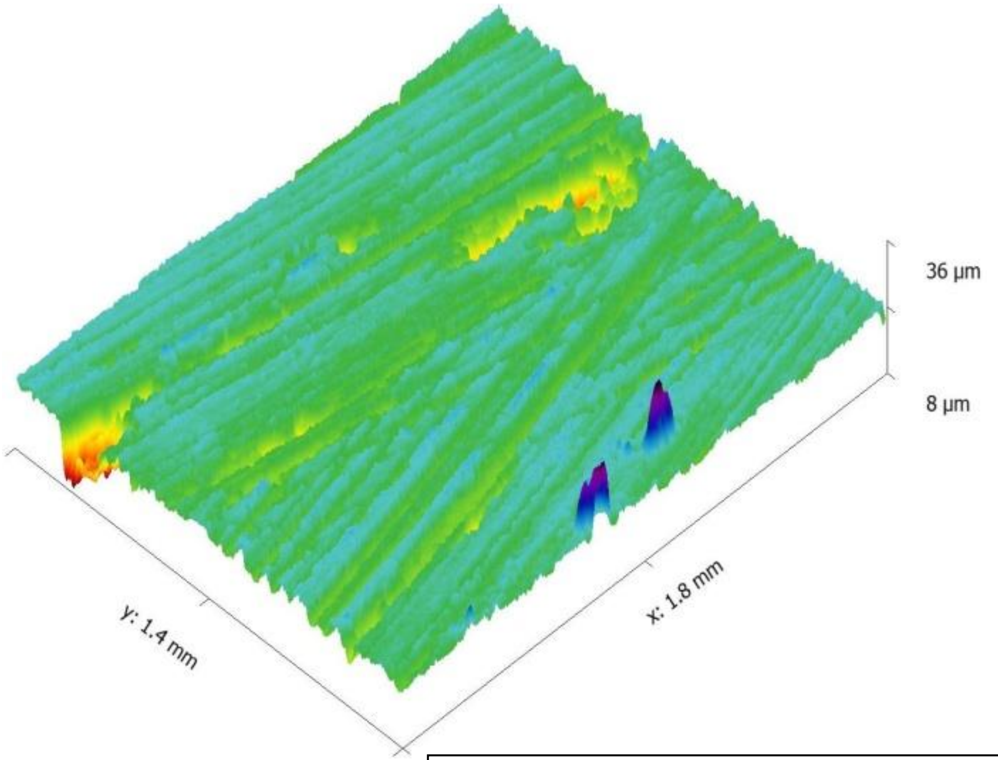

Surface roughness (R_a=0.51µm)

Figure 4.19: Worn surface topography of the stirred MMC subjected to the SIMA process at 40 N load and 1 m/s sliding is sliding velocity under SEM and profilometer

4.4 Conclusions

The present work concerns with semi-solid processing of Al-10Cu alloy following SIMA process. A cast alloy was subjected to warm working at 300 ºC and intercritically annealed at 580 ºC in two phase solid-liquid region. The result revealed accelerated spheroidization of the primary α- phase. The size of the spheroids varied from 45 to 65 µm.

The casting process carried out from the melt subjected to vigorous stirring prior to pouring into the mold followed by SIMA processing revealed uniform distribution of solutes in the matrix phase. Hence, it is exhibited a low wear rate compared to metal mould cast alloy and metal mould cast alloy subjected to the SIMA processing technique.

The hardness (156 HV) and UTS (223 MPa) were observed to be higher in the stirred metal mould cast alloy subjected to SIMA process. Analysis of wear track surfaces brought out a clear evidence of co-existing abrasion and adhesion mechanisms of material removal during tribological study of SIMA processed alloy.

The wear rate and coefficient of friction of this stirred MMC subjected SIMA process are lower because of the higher hardness value of 156.2 HV, the higher ultimate tensile strength (223.8 MPa) and a finer grain size (45 µm) compared with the MMC and MMC subjected to the SIMA process of the same alloy.